Medizinische Fakultät
der
Universität Duisburg-Essen

Aus der Klinik für Kinderheilkunde I

Tumor necrosis factor-inducible gene 6 protein: A novel neuroprotective factor against inflammation-induced developmental brain injury

I n a u g u r a l – D i s s e r t a t i o n
zur
Erlangung des Doktorgrades der Medizin
durch die Medizinische Fakultät
der Universität Duisburg-Essen

Vorgelegt von
Frederik Bertling
aus Stadtlohn
11.01.2017

Dekan:		Herr Univ.-Prof. Dr. med. J. Buer
1.	Gutachter:	Frau Univ.-Prof. Dr. med. U. Felderhoff-Müser
2.	Gutachter:	Herr Univ.-Prof. Dr. med. D. Hermann
3.	Gutachter:	Herr Prof. Dr. med. Dr. h.c. K. Unsicker, Freiburg

Tag der mündlichen Prüfung: 12. September 2017

Publikationen

Bertling, F., Bendix, I., Drommelschmidt, K., Wisniewski, H., Felderhoff-Mueser, U., Keller, M., Prager, S. (2016):
Tumor necrosis factor-inducible gene 6 protein: A novel neuroprotective factor against inflammation-induced developmental brain injury.
Experimental Neurology 279, 283–289.

Prager, S., Singer, B.B., Bendix, I., Schlager, G.W., Bertling, F., Ceylan, B., Keller, M., Felderhoff-Mueser, U., Ergün, S. (2013):
CEACAM1 expression in oligodendrocytes of the developing rat brain shows a spatiotemporal relation to myelination and is altered in a model of encephalopathy of prematurity.
Dev Neurosci. 35, 226–240.

Drommelschmidt, K., Serdar, M., Bendix, I., Herz, J., Bertling, F., Prager, S., Keller, M., Ludwig, A., Duhan, V., Radtke, S., de Miroschedji, K., Horn, P.A., van de Looij, Yohan., Giebel, B., Felderhoff-Mueser, U. (2017):
Mesenchymal stem cell-derived extracellular vesicles ameliorate inflammation-induced preterm brain injury.
Brain, Behavior, and Immunity 60, 220-232

Für meine Familie

Contents

1. Introduction

1.1. Definition of preterm birth

Preterm birth is defined as birth before the 37th week of gestation. Therefore the term ”preterm birth” subsumes a heterogeneous group of newborns that includes babies born nearly at term, but also those that are born as early as 22 weeks of gestational age. To categorize this group in more homogeneous subgroups, two different approaches were established: categorization by gestational age and categorization by birth weight. Categorization by gestational age results in the subgroups listed below (Goldenberg et al., 2008; Saigal, Doyle, 2008):

- 34 0/7 - 36 6/7 weeks (late prematurity) - 60-70%
- 32 0/7 - 33 6/7 weeks (moderate prematurity) - 20%
- 28 0/7 - 31 6/7 weeks (severe prematurity) - 15%
- $<$28 weeks (extreme prematurity) - 5%

Nonetheless, birth weight is not only related to gestational age, as there are newborns which are small for gestational age (SGA), e.g. because of intrauterine growth restriction (IUGR). Therefore, many studies dealing with preterm birth also use the following categorization (Gill et al., 2013):

- $<$2500 g Low Birth Weight (LBW)
- $<$1500 g Very Low Birth Weight (VLBW)
- $<$1000 g Extremely Low Birth Weight (ELBW)

1.2. Epidemiology and relevance of preterm birth

135 million babies are born each year, 15 million of them are preterms (Lawn et al., 2013). In Europe, the amount of preterm birth among all births was also increasing in recent years, currently varying between 6.3% (Sweden, France) and 11.4% (Austria) (Keller et al., 2010). The report for disability-adjusted life years, based on data from the Global Burden of Disease Study 2010, ranks preterm birth complications at #8 worldwide, which is an improvement compared to #3 in 1990. Statistics for years of life lost show similar results with a change from #3 in 1990 to #7 in 2010 (Murray et al., 2012). Thus, modern therapeutic strategies and social programs, most prominently the millennium development goals, have achieved significant improvements. Nevertheless, the impact of preterm birth complications on global health is still very high and requires further improvements.

While mortality of babies from Africa is mainly caused by infectious diseases (41%), preterm birth has climbed to the peak in industrialized areas, like North America and Europe (42%, 38%) (Lawn et al., 2006). Adjusted to the neonatal mortality rate (NMR), the percentage of preterm and congenital reasons is growing while infectious reasons are decreasing the lower the NMR is (Lawn et al., 2005). Therefore, with economic improvements in poor countries, we can expect the NMR to decrease with subsequent increase of the proportion of preterm birth in neonatal mortality.

1.3. Aetiology and pathophysiology of preterm birth

Preterm birth is induced by many foetal and maternal factors (Villar et al., 2012). A well-known mechanism is infection/inflammation, also called microbial invasion of the amniotic cavity (MIAC), for which a firm causal link and a molecular pathophysiology was described (Romero et al., 2007). Its percentage as a trigger for preterm birth is estimated to be 25%-40%, which may even be an underestimation because intrauterine infections are difficult to detect with conventional culture techniques and are mostly subclinical. Additionally, the lower the gestational age at birth, the higher is the rate of MIAC of the mothers (Romero et al., 2006).

1.4. Preterm birth associated morbidity

Even though the rate of preterm birth is increasing among neonatal mortalities, overall mortality has declined over the past three decades. With increasing survival rates of immature neonates, the absolute number of babies suffering morbidity is rising (Wen et al., 2004; Saigal, Doyle, 2008). The organs most affected by prematurity are the brain (encephalopathy of prematurity)(Rees, Inder, 2005), the lungs (Jobe, Bancalari, 2001), the gut and the retina (Zeitlin et al., 2016). In our work, we focus on the brain, as encephalopathy of prematurity is essential for long-term prognosis.

1.4.1. Encephalopathy of prematurity

Encephalopathy of prematurity summarizes two severe neurological disorders: Periventricular Leukomalacia (PVL) and neuronal/axonal disease (Volpe, 2009).

Periventricular Leukomalacia PVL refers to injury of cerebral white matter, especially periventricular, i.e. the white matter adjacent to the ventricles. The injury consists of focal necrotic lessions, which can be observed macroscopically (cystic PVL) or only microscopically (non-cystic PVL) and a more diffuse injury surrounding these lesions. The term PVL was introduced by morphological observations of Rudolf Virchow in 1867 (Virchow, 1867). Today, we know that histological changes observed are caused by astrogliosis, microgliosis and most importantly, by a decrease in premyelinating oligodendrocytes. This is counteracted by an increase in oligodendroglial progenitors. However, these progenitors seem to lack the

capability to differentiate to mature myelin producing cells, resulting in a hypomyelination of the white matter (Volpe, 2009).

Neuronal/axonal disease Neuronal/axonal disease describes a reduced volume of grey matter structures, such as the thalamus, basal ganglia, cerebral cortex, and cerebellar cortex and nuclei. The reduced volume persists until adulthood. It often occurs in combination with PVL (Volpe, 2009).

1.4.1.1. Epidemiology, aetiology and outcome

Long-term equivalents of encephalopathy of prematurity are motor deficits, cerebral palsy, sensory impairments of the auditory and visual system, mental disability, autism and schizophrenia (Hagberg et al., 2012; Larroque et al., 2008; Saigal, Doyle, 2008). Its aetiology is multi-factorial with the following underlying causes: drugs, hypoxia & ischaemia, hyperoxia, hypocarbia and inflammation (Hagberg, Mallard, 2005; Degos et al., 2010; Deng, 2010).

Even though late preterms account for 60%-70% of all prematurely born infants and moderate preterms contribute with 20%, most studies emphasize on preterm birth before the 32th week of gestation, because they suffer the most from morbidity (Kramer et al., 2000). In a Swedish study from 1999-2002, the prevalence of cerebral palsy, which can be considered to be the most severe motor disorder, was 2.18‰. The age-specific prevalences were 55.6‰ for children born before the 28th week of gestation, 43.7‰ for children born at 28th-31th week, 6.1‰ for children born at 32th-36th week and 1.43‰ for children born at term (Himmelmann et al., 2010). A study from Utrecht, The Netherlands, from 1990 to 2005 revealed that the prevalence of cerebral palsy in children born before the 34th week of gestation (mean = 30.2) has declined from 6.5% to 2.2%, which was almost exclusively attributed to a reduction of severe cystic PVL (Haastert et al., 2011).

1.4.1.2. Inflammation as a causal factor

Infection and/or inflammation do not only contribute to preterm birth with 25%-40%, they are also well-known risk factors for encephalopathy of prematurity (Hagberg, Mallard, 2005; Degos et al., 2010; Deng, 2010). Therefore they do not only aggravate the already increased risk of preterms to develop encephalopathy of prematurity, but also contribute to neurological disorders of term babies. A meta-analysis of studies investigating the effect of chorioamnionitis on cerebral palsy revealed that the attributable risk is 12% for normal-birth-weight children and 28% for premature infants (Wu, Colford, 2000). The complexity of the underlying pathophysiology required the development of suitable animal models (Burd et al., 2012).

LPS A variety of animal studies used lipopolysaccharide (LPS) to model the systemic inflammatory response induced by infections. LPS is part of the outer membrane of gram-negative bacteria and effectively triggers the innate immune system. The recognition of LPS starts with binding to LPS-binding protein (LBP), an acute-phase protein. It circulates in the bloodstream and forms a complex with LPS, which promotes the subsequent binding to cell

surface receptors. Two pathways have been identified to be involved in LPS recognition: TLR-2 and TLR-4. CD-14 enhances the LPS response of TLR-2. CD-14 and MD-2 are acting as adapter-molecules for TLR-4. TLR-2 and TLR-4 finally transduce the signal across the cell membrane. Both pathways result in nuclear translocation of NF-κB promoting transcription of various inflammatory genes (Pålsson-McDermott, O'Neill, 2004; Godowski et al., 1998).

Expansion to a systemic response An acute-phase liver response (APR) is then triggered by secretion of pro-inflammatory cytokines, especially TNF-α , IL-1 and IL-6. The APR promotes systemic inflammation by secretion of further cytokines, prostaglandins and by activation of the complement and fibrinolytic systems. Furthermore, cells of the immune system, like polymorphonuclear leukocytes and monocytes, are recruited from the bone marrow. These processes already lead to reactions from the central nervous system (CNS), like 'sickness behaviour', neuroendocrine and metabolic changes, activation of the hypothalamic-pituitary-adrenal axis and increased catabolism. Thus the CNS must interact in some way with the systemic inflammatory response (Hagberg, Mallard, 2005).

Involvement of the CNS The cross-talk between bloodstream and CNS is mostly controlled by the blood brain barrier (BBB). It is formed by special endothelial cells and exhibits a very low permeability to cells and proteins. The circumventricular organs (CVO) do not exhibit a BBB and therefore show higher permeability to cells and proteins (Fry, Ferguson, 2007). Interestingly, subseptic low doses of LPS (0.01-10 µg/kg) induced expression of IL-1β and TNF-α mRNA only in the CVOs and the meninges, while higher doses ($>$500 µg/kg) induce global expression of pro-inflammatory cytokines in the whole brain, at least in adult rats (Quan et al., 1999). Thus, the differences in the BBB of different brain regions also demonstrate diverse reaction thresholds on inflammation. But, as the maturation of the BBB is not completed in neonates, it remains unclear whether adult results can be translated to the neonatal brain (Semple et al., 2013).

From neuroinflammation to neuronal damage Both white matter damage and grey matter damage are observed in preterm infants with encephalopathy of prematurity. Ådén et al. reported that systemic inflammation leads to neuroinflammation with increased cytokine expression and microglia activation. The white matter as the predominating area of injury suffers from increased vulnerability of pre-oligodendrocytes (preOLGs) to oxidative stress, most likely because of their high dependency on gluthation for protection against free radicals, compared to both mature oligodendrocytes and astrocytes (Oka et al., 1993; Back et al., 1998). Predominantley the so called excitotoxicity, caused by high levels of extracellular glutamate with subsequent transporter-triggered intracellular cystine depletion, which is an essential part of gluthation, stresses the gluthation dependency of preOLGs. Furthermore, high levels of extracellular glutamate activate α-amino-3-hydroxy-5-methyl-4-isoxazolepropionic acid (AMPA) and kainate receptors to increase Ca^{2+} influx in late oligodendrocyte progenitor cells, resulting in cell death. Even though excitotoxicity is mostly described in hypoxic/ischaemic white matter injury by energy depletion, dying or dead cells in inflammation-induced white

matter injury also release glutamate into the extracellular milieu (Deng, 2010; Liu et al., 2013; Hagberg et al., 2015).

The reasons for grey matter damage are less clear, but two mechanisms are under debate: 1) Damage to axons in the white matter can lead to retrograde degeneration of projecting neurons. 2) The immature brain exhibits neurons in the white matter, which later migrate to their destination and are reduced in white matter injury (Volpe, 2011).

1.4.1.3. Therapeutic strategies

Current treatment aims at prevention, because a therapeutic approach to specifically tackle the pathophysiology of inflammation-induced developmental brain injury is not yet available (Favrais et al., 2014; Hagberg et al., 2015). Interestingly, mesenchymal stem cells (MSC) have been proposed to be beneficial in many inflammatory diseases, including developmental brain injury (Castillo-Melendez et al., 2013). MSCs secrete the anti-inflammatory protein Tumor-necrosis factor inducible gene 6 (TSG-6), which has been suggested to be responsible for a significant part of the beneficial effects of MSCs.

1.5. TSG-6: an endogenous protein with anti-inflammatory activity

Since TSG-6 was discovered in TNF-α stimulated fibroblasts in 1990 (Lee et al., 1990), its structure and function was intensively investigated (Milner, Day, 2003; Milner et al., 2006). Its pathophysiological role as an anti-inflammatory mediator in arthritis was discovered earlier (Wisniewski et al., 1993; Wisniewski et al., 1996). A physiological role of TSG-6 during ovulation by expanding the extracellular matrix of the cumulus oophorus complex was investigated in the late 90ies (Fülöp et al., 1997; Fülöp et al., 2003; Richards, 2005). Additionally, a relevance for TSG-6 in maintaining the physiological architecture of skin was described recently (Tan et al., 2011). Further studies demonstrated a therapeutic potential of TSG-6 in several inflammatory conditions: myocardial infarction (Lee et al., 2009), acute lung injury (Danchuk et al., 2011) and corneal injury (Oh et al., 2010).

Multiple functions of TSG-6 have been implied. It strongly influences the extracellular matrix by catalysing the formation of Hyaluronan-Heavychain complexes (Rugg et al., 2005; Sanggaard et al., 2008; Sanggaard et al., 2010), creating condensed Hyaluronan matrices *in vitro* (Baranova et al., 2011). It also modulates the anti-plasmin activity of the bikunin domain of inter-α-inhibitor, which is abundant in plasma (Wisniewski et al., 1996). Effects which emphasize the anti-inflammatory potential of TSG-6 are its ability to inhibit neutrophil migration (Getting et al., 2002) and its capability to influence inflammatory mediators, e.g. by up-regulation of COX-2 expression with subsequent secretion of PGD_2 (Mindrescu et al., 2005) and by CD-44 dependent inhibition the TLR-2 signal cascade limiting the amount of translocated NF-κB into the cell nucleus (Choi et al., 2011).

To date the role of TSG-6 in the developing brain remains unclear.

1.6. Hypothesis and aims

Preterm birth with subsequent inflammation-induced developmental brain injury is a highly prevalent burden for society (1.2, 1.4.1.1) with unsatisfying prevention capabilities because intrauterine infection as its main factor is commonly subclinical and difficult to detect by conventional culture techniques (1.3). Therefore it is mandantory to develop therapeutic strategies which are currently not available (1.4.1.3). Interestingly, mesenchymal stem cells (MSC) have been proposed to be beneficial in many inflammatory diseases, including developmental brain injury (Castillo-Melendez et al., 2013). MSCs secrete the anti-inflammatory protein Tumor-necrosis factor inducible gene 6 (TSG-6), which has been suggested to be responsible for a significant part of the beneficial effects of MSCs (1.4.1.3). Because of the the anti-inflammatory effects of TSG-6 under several inflammatory conditions, we postulate that TSG-6 might be beneficial in inflammation-induced developmental brain injury as well. The aims of the current study were to evaluate 1) the developmental expression of TSG-6 in the neonatal rat brain, 2) the role of TSG-6 in perinatal inflammation with special focus on neuroinflammation in the neonatal rat brain, and 3) the effect of exogenous administration of TSG-6 on inflammation-induced developmental brain injury using an established rat model (Prager et al., 2013; Brehmer et al., 2012).

The Developmental expression of TSG-6 in the neonatal rat brain TSG-6 was heavily investigated in the last 25 years but its physiological functions are still mainly unkown (1.5). In order to gain insight into a possible role of TSG-6 in the neonatal rat brain and to understand putative implications for an exogenous administration of TSG-6, we aim to evaluate the developmental expression of TSG-6 in the neonatal rat brain.

The role of TSG-6 in perinatal inflammation As TSG-6 is an endogenous protein with anti-inflammatory activity, it is most likely expressed to counteract inflammation (1.5). In order to gain insight into a possible role of TSG-6 in neonatal neuroinflammation and to understand putative implications for an exogenous administration of TSG-6, we aim to evaluate the expression of TSG-6 in the neonatal rat brain under neuroinflammatory conditions.

The effect of exogenous TSG-6 on inflammation-induced developmental brain injury Finding a treatment for inflammation-induced developmental brain injury is of great interest for our society. Our final aim is to evaluate if exogenous TSG-6 is an appropriate substance in treatment of inflammation-induced developmental brain injury.

2. Materials and methods

2.1. Materials

2.1.1. Laboratory animals

Wistar rats were used for all animal experiments. Their breeding and keeping is uncomplicated, and they genetically and anatomically resemble humans. Furthermore, key developmental processes in brain development of preterm infants occur in rodents in the early postnatal days, known as the brain growth spurt (Dobbing, Sands, 1979). These processes are oligodendrocyte maturation state changes, neuronal sprouting and formation of synapses, immune system development and establishment of the BBB. These events are especially important in inflammation-induced developmental brain injury (Semple et al., 2013). All animal experiments were performed in accordance with international guidelines for good laboratory practice and institutional guidelines of the University Hospital Essen and were approved by the animal welfare committees of North Rhine Westphalia (ID: G 1111/10).

2.1.2. Chemicals

Item	Manufacturer
anti-Human TSG-6 Affinity Purified Polyclonal Ab, Goat IgG #AF2104	R&D Systems, Minneapolis, MN 55413, USA
anti-TSG-6 Antibody (E-10)	Santa Cruz Biotechnology Inc., 69115 Heidelberg, Germany
anti-TSG-6 Antibody (FL-277)	Santa Cruz Biotechnology Inc., 69115 Heidelberg, Germany
Monoclonal Anti-β-Actin antibody	Sigma-Aldrich Chemie GmbH, 82024 Taufkirchen, Germany
anti-GAPDH Antibody (FL-335)	Santa Cruz Biotechnology Inc., 69115 Heidelberg, Germany
anti-Cleaved Caspase-3 (Asp175) (5A1E) Rabbit mAb #9664L	Cell Signaling Technology, Danvers, MA 01923, USA

Anti Iba1, Rabbit Cat. No. 016-20001	Wako Pure Chemical Industries, Ltd, 1-2 Doshomachi 3-Chome, Chuo-ku, Osaka 540-8605, Japan
Anti-rabbit IgG, HRP-linked Antibody #7074	Cell Signaling Technology, Danvers, MA 01923, USA
Polyclonal Rabbit Anti-Goat Immunoglobulins/HRP	Dako Deutschland GmbH, Hamburg 22083, Germany
Goat anti-Rabbit IgG (H+L) Secondary Antibody, Alexa Fluor® 594 conjugate	Thermo Fisher Scientific, Waltham, MA 02454, USA
Goat anti-Mouse IgG (H+L) Secondary Antibody, Alexa Fluor® 594 conjugate	Thermo Fisher Scientific, Waltham, MA 02454, USA
Rabbit anti-Goat IgG (H+L) Secondary Antibody, Alexa Fluor® 594 conjugate	Thermo Fisher Scientific, Waltham, MA 02454, USA
Polyclonal Goat Anti-Rabbit Immunoglobulins/Biotinylated	Dako Deutschland GmbH, Hamburg 22083, Germany
Polyclonal Goat Anti-Mouse Immunoglobulins/Biotinylated	Dako Deutschland GmbH, Hamburg 22083, Germany
Polyclonal Rabbit Anti-Goat Immunoglobulins/Biotinylated	Dako Deutschland GmbH, Hamburg 22083, Germany

Table 2.1.: Antibodies

Item	Manufacturer
TSG-6 forward primer, GTA GGA AGA TAC TGC GGT GAT GAA	BioTeZ Berlin-Buch GmbH, 13125 Berlin, Germany
TSG-6 reverse primer, GAC GGA CGC ATC ACT CAG AA	BioTeZ Berlin-Buch GmbH, 13125 Berlin, Germany
TSG-6 probe, 6-FAM – TCC AGA AGA CAT CAT CAG CAC AGG AAA TGT – BHQ1	BioTeZ Berlin-Buch GmbH, 13125 Berlin, Germany
GAPDH forward primer, GAT GCT GGT GCT GAG TAT GTC GT	BioTeZ Berlin-Buch GmbH, 13125 Berlin, Germany
GAPDH reverse primer, TCA GGT GAG CCC CAG CCT	BioTeZ Berlin-Buch GmbH, 13125 Berlin, Germany
GAPDH probe, 6-FAM – TCT ACT GGC GTC TTC ACC ACC ATG GAG A – BHQ1	BioTeZ Berlin-Buch GmbH, 13125 Berlin, Germany
Ubiquitin C forward primer, CCG GCG GGC ACT GAT	BioTeZ Berlin-Buch GmbH, 13125 Berlin, Germany
Ubiquitin C reverse primer, CAT TTT TAA CAG AGG TTC AGC TAT TAC TG	BioTeZ Berlin-Buch GmbH, 13125 Berlin, Germany

Ubiquitin C probe, 6-FAM – CAT TAC TCT GCA CTC TAG CCA TTT GCC CC – BHQ1	BioTeZ Berlin-Buch GmbH, 13125 Berlin, Germany

Table 2.2.: Primer

Item	Manufacturer
Milk powder Blotting grade	Carl Roth GmbH + Co. KG, 76185 Karlsruhe, Germany
Chloral hydrate C-IV	Sigma-Aldrich Chemie GmbH, 82024 Taufkirchen, Germany
Ammonium persulfate for molecular biology	AppliChem GmbH, 64291 Darmstadt, Germany
Paraformaldehyde	Sigma-Aldrich Chemie GmbH, 82024 Taufkirchen, Germany
Sodium Chloride	AppliChem GmbH, 64291 Darmstadt, Germany
Glycin for molecular biology	AppliChem GmbH, 64291 Darmstadt, Germany
Tris for molecular biology	AppliChem GmbH, 64291 Darmstadt, Germany
cOmplete Mini, EDTA-free	Roche Diagnostics Deutschland GmbH, 68305 Mannheim, Germany
Ponceau S	ICN Biomedicals Inc, 37269 Eschwege, Germany
Nuclear fast red for microscopy	Merck KGaA, 64293 Darmstadt, Germany
Aluminium sulfate 18-hydrate	Merck KGaA, 64293 Darmstadt, Germany
111374 Buffer tablets pH 6.8	Merck KGaA, 64293 Darmstadt, Germany

Table 2.3.: Solid substances

Item	Manufacturer
NaCl 0.9%	B. Braun Melsungen AG, 34209 Melsungen, Germany
Lipopolysaccharide from Escherichia coli Serotype 0111:B4	Sigma-Aldrich Chemie GmbH, 82024 Taufkirchen, Germany
LiChrosolv®	Merck KGaA, 64293 Darmstadt, Germany
99%, p.a., N,N,N',N'-Tetramethylethylendiamin	Carl Roth GmbH + Co. KG, 76185 Karlsruhe, Germany
Chloroform for analysis	AppliChem GmbH, 64291 Darmstadt, Germany
Phenylmethanesulfonylfluoride solution	Sigma-Aldrich Chemie GmbH, 82024 Taufkirchen, Germany
Methanol AnalaR NORMAPUR Reagenz Ph. Eur.	VWR International GmbH, 64295 Darmstadt, Germany
Ethanol absolut AnalaR NORMAPUR	VWR International GmbH, 64295 Darmstadt, Germany
2-Propanol, for molecular biology, $\geq$ 99%	Sigma-Aldrich Chemie GmbH, 82024 Taufkirchen, Germany
SDS-Solution 20%	AppliChem GmbH, 64291 Darmstadt, Germany
2-Mercaptoethanol min. 98%	Sigma-Aldrich Chemie GmbH, 82024 Taufkirchen, Germany
Eukitt®	ORSAtec GmbH Niederlassung Bobingen, 86399 Bobingen, Germany
Xylene - Mixture of isomeres (Reag. Ph. Eur.) for analysis, ACS, ISO C	AppliChem GmbH, 64291 Darmstadt, Germany
101424 May-Grünwald's eosine-methylene blue solution modified	Merck KGaA, 64293 Darmstadt, Germany
109204 Giemsa's azur-eosin-methylene blue	Merck KGaA, 64293 Darmstadt, Germany
Tween® 20 Pure	SERVA Electrophoresis GmbH, 69115 Heidelberg, Germany
TRIzol® Reagent	Life Technologies, Carlsbad, CA 92018, USA

Acetic acid (glacial) 100%	Merck KGaA, 64293 Darmstadt, Germany
RIPA buffer	Sigma-Aldrich Chemie GmbH, 82024 Taufkirchen, Germany
Precision Plus Protein Standards Dual Color	Bio-Rad Laboratories GmbH, 80901 München, Germany
Rotiphorese® Gel 30	Carl Roth GmbH + Co. KG, 76185 Karlsruhe, Germany
Fluorescence Mounting Medium	Dako Deutschland GmbH, Hamburg 22083, Germany
Aqua ad iniectabilia	B. Braun Melsungen AG, 34209 Melsungen, Germany

Table 2.4.: Fluids

Item	Manufacturer
Amersham ECL Plus	GE Healthcare, 42655 Solingen, Germany
DNase I Amplification Grade	Life Technologies, Carlsbad, CA 92018, USA
SuperScript® II Reverse Transcriptase	Life Technologies, Carlsbad, CA 92018, USA
Random Primers	Life Technologies, Carlsbad, CA 92018, USA
TaqMan® Fast Universal PCR Master Mix (2x)	Thermo Fisher Scientific, Waltham, MA 02454, USA
BCA® Protein Assay Kit	Thermo Fisher Scientific, Waltham, MA 02454, USA
Bio-Plex Pro™ Rat Cytokine Assay	Bio-Rad Laboratories GmbH, 80901 München, Germany
VECTASTAIN ABC HRP Kit (Peroxidase, Standard)	Vector Laboratories, Burlingame, Ca 94010, USA
Bio-Plex® Cell Lysis Kit	Bio-Rad Laboratories GmbH, 80901 München, Germany

DAB Peroxidase (HRP) Substrate Kit (with Nickel), 3,3'-diaminobenzidine	Vector Laboratories, Burlingame, Ca 94010, USA

Table 2.5.: Kits

2.1.3. Buffers and solutions

2.1.3.1. General solutions

- Phosphat buffered saline (PBS), pH 7.4
  - 137 mM NaCl
  - 2.7 mM KCl
  - 12 mM phosphate
  - Titrate to pH 7.4 with HCl
- Tris buffered saline (TBS), pH 7.4
  - 100 mM Tris
  - 300 mM NaCl
  - Titrate to pH 7.4 with HCl
- Tris buffered saline with Tween (TBS-T), pH 7.4
  - 100 mM Tris
  - 300 mM NaCl
  - 0.1% Tween 20
  - Titrate to pH 7.4 with HCl
- 4% Paraformaldehyde (PFA) in PBS, pH 7.4
  - 4% PFA
  - PBS
  - Titrate to pH 7.4 with HCl

2.1.3.2. Solutions for gelelectrophoresis

- Electrophoresis buffer
  - 0.192 M glycine
  - 0.1% SDS
  - 25 mM Tris
  - Titrate to pH 8.1 with HCl
- Transfer buffer

  - 25 mM Tris
  - 114 mM glycine
  - 20% methanol

- Stacking gel 4.5%
  - 3.7 ml 4x stacking gel buffer
    - 0.4% SDS
    - 0.5 M Tris
    - Titrate to pH 6.8 with HCl
  - 2.2 ml Rotiphorese® Gel 30
  - 9 ml H_2O
  - 50 µl APS 12.5%
  - 30 µl TEMED
- Separating gel 12.5%
  - 6 ml 4x separating gel buffer
    - 0.4% SDS
    - 1.5 M Tris
    - Titrate to pH 8.8 with HCl
  - 10 ml Rotiphorese® Gel 30
  - 7.9 ml H_2O
  - 96 µl APS 12.5%
  - 20 µl TEMED
- Laemmli buffer 2x
  - 2.5 ml 0.5 M Tris
  - 2 ml SDS 20%
  - 2 ml 87% glycerol
  - 0.5 ml β-mercaptoethanol
  - 3 ml H_2O
  - Some crumbs of bromophenol blue
  - Titrate to pH 6.8 with HCl
- Ponceau S solution
  - 0.1% Ponceau S
  - 5% acetic acid

2.1.3.3. Solutions for real-time PCR

- DNAse Master Mix
  - 1 µl DNAses
  - 1 µl DNAses 10x Buffer
  - 8 µl H_2O/RNA mix to reach a total concentration of 100 ng/µl
- RT Master Mix I
  - 1 µl oligo dTs
  - 1 µl dNTPs
  - 1 µl random primers
  - 2 µl H_2O
- RT Master Mix II
  - 4 µl First Strand Buffer 5x
  - 2 µl 0.1 M DTT
  - 1 µl SuperScript II
  - 3 µl H_2O

2.1.3.4. Solutions for immunohistochemistry

- Citrate buffer
  - 10 mM tri-sodium citrate
  - 0.05% Tween 20
  - Titrate to pH 6.0 with HCl
- H_2O_2/methanol solution
  - 0.3% H_2O_2
  - 70% methanol
  - TBS
  - keep away from light
- ABC solution
  - 5 ml PBS
  - 2 drops ABC kit fluid A
  - 2 drops ABC kit fluid B
  - prepare 30 min before use
- DAB solution
  - 5 ml H_2O

  - 2 drops DAB kit buffer stock solution
  - 4 drops DAB kit DAB stock solution
  - 2 drops DAB kit hydrogen peroxide solution
  - 2 drops DAB kit nickel
- Nuclear fast red solution
  - 5 g aluminium sulfate
  - 100 ml H_2O
  - Heat aluminium sulfate and H_2O to 100 °C and add 0.1 g nuclear fast red until its dissolves. Cool down afterwards.
- DAPI-PBS solution
  - 360.59 nM DAPI
  - PBS pH 7.4

2.1.3.5. Several blocking buffers

- Immunohistochemistry (IHC)
  - 50 mM Tris
  - 0.9% NaCl
  - 0.3 g FSG
  - 1 g BSA
  - Titrate to pH 7.6 with HCl
- Western blot (WB)
  - 0.1% milk powder
  - 20 mM Tris
  - 500 mM NaCl
  - Titrate to pH 7.5 with HCl
- Milk powder (MP)
  - 5% milk powder
  - TBS-T

2.1.4. Equipment

Device	Manufacturer
NanoDrop 1000 Spectrophotometer	NanoDrop products, Wilmington, DE 19810, USA
Infinite M200	Tecan Group Ltd., 8708 Männedorf, Switzerland
StepOne Plus	Thermo Fisher Scientific, Waltham, MA 02454, USA
Maxigel	Biometra GmbH, 37079 Göttingen, Germany
T3 Thermocycler	Biometra GmbH, 37079 Göttingen, Germany
PowerPac HC Power Supply	Bio-Rad Laboratories GmbH, 80901 München, Germany
Criterion Blotter	Bio-Rad Laboratories GmbH, 80901 München, Germany
Bio-Plex Handheld Magnetic Washer	Bio-Rad Laboratories GmbH, 80901 München, Germany
ChemiDoc XRS+ System	Bio-Rad Laboratories GmbH, 80901 München, Germany
Avanti 30 Centrifuge	Beckman Coulter GmbH, 47807 Krefeld, Germany
HLC HeizThermoMixer MHR 23	DITABIS AG, 75179 Pforzheim, Germany
Thermomixer 5436	Eppendorf AG, 22339 Hamburg, Germany
Centrifuge 5417R	Eppendorf AG, 22339 Hamburg, Germany
Tissue Embedding System TES 99	MEDITE GmbH, 31303 Burgdorf, Germany
LUMINEX® 200™	Luminex Corporation, 5215 MV ‘s-Hertogenbosch, The Netherlands
Microm HM 430	Thermo Fisher Scientific, Waltham, MA 02454, USA

HIR-3	KUNZ INSTRUMENTS AB, 149 30 Nynashamn, Sweden
Axioplan	Carl Zeiss AG, 73447 Oberkochen, Deutschland
Forma 900 Series	Thermo Fisher Scientific, Waltham, MA 02454, USA
Routine meter pH 526	Sigma-Aldrich Chemie GmbH, 82024 Taufkirchen, Germany
PCB 1000-2	KERN & SOHN GmbH, 72336 Balingen-Frommern, Deutschland
Rotilabo®-mini-centrifuge	Carl Roth GmbH + Co. KG, 76185 Karlsruhe, Germany
Minishaker MS2	IKA®-Werke GmbH & CO. KG, 79219 Staufen, Germany
Microwave Y53	Krups GmbH, 60554 Frankfurt am Main, Germany
Shandon™ Sequenza™ Immunostaining Center Accessories	Thermo Fisher Scientific, Waltham, MA 02454, USA
Colibri.2	Carl Zeiss AG, 73447 Oberkochen, Deutschland
AxioCam ICc1	Carl Zeiss AG, 73447 Oberkochen, Deutschland

Table 2.6.: Equipment

2.1.5. Instruments

Instrument	Manufacturer
100 µl Hamilton-Pipette (710n 22s/51/2)	Hamilton Robotics, CH-7402 Bonaduz, GR, Switzerland
Research® 1000 µl/200 µl/100 µl/20 µl/10 µl	Eppendorf AG, 22339 Hamburg, Germany
edding 3000 permanent marker blue/green	edding Vertrieb GmbH, 31515 Wunstorf, Germany
Fisherbrand™ Glass Staining Dishes	Thermo Fisher Scientific, Waltham, MA 02454, USA

pipetus®	Hirschmann Laborgeräte GmbH & Co. KG, 74246 Eberstadt Germany
Multipette® Stream	Eppendorf AG, 22339 Hamburg, Germany

Table 2.7.: Instruments

2.1.6. Disposables

Instrument	Manufacturer
1.5 ml/2.0 ml reaction tubes	Eppendorf AG, 22339 Hamburg, Germany
15 ml/ 50 ml conical centrifuge tubes	Greiner Bio-One GmbH, 72636 Frickenhausen, Germany
5 ml/10 ml/25 ml serological pipette	Greiner Bio-One GmbH, 72636 Frickenhausen, Germany
10 µl/200 µl/1000 µl TipOne® sterile filter tips	STARLAB GmbH, 22143 Hamburg, Germany
Amersham Protran 0.45 µm/0.2 µm NC	GE Healthcare, 42655 Solingen, Germany
Rotilabo®-Blotting papers, 1.5mm	Carl Roth GmbH + Co. KG, 76185 Karlsruhe, Germany
MicroAmp® Optical Adhesive Film	Thermo Fisher Scientific, Waltham, MA 02454, USA
96x0.2 ml Plate	BIOplastics, 6374 XW Landgraaf, The Netherlands
my-Budget 8er-Strips	Bio-Budget Technologies GmbH, 47805 Krefeld, Deutschland
Corning®, Costar® 96 Well Cell Culture Cluster	Sigma-Aldrich Chemie GmbH, 82024 Taufkirchen, Germany
SuperFrost® Plus slides	R. Langenbrinck Labor- und Medizintechnik, 79312 Emmendingen, Germany
Slides 76x26 mm	Engelbrecht Medizin- und Labortechnik GmbH, 34295 Edermündey, Germany

Cover slides 24 x 60 mm	Engelbrecht Medizin- und Labortechnik GmbH, 34295 Edermündey, Germany
GK 150 EDTA 200 µl	KABE LABORTECHNIK GmbH, 51588 Nümbrecht-Elsenroth, Germany
Shandon™ Glass Coverplates	Thermo Fisher Scientific, Waltham, MA 02454, USA
Rotilabo®-embedding cassettes, Macro	Carl Roth GmbH + Co. KG, 76185 Karlsruhe, Germany
BD Eclipse™ 30G 1/2“	BD, 69126 Heidelberg, Germany
BD Plastipak™ 1 ml	BD, 69126 Heidelberg, Germany

Table 2.8.: Disposables

2.2. Methods

2.2.1. Animal model

Wistar rats were kept in the central animal facility of the University Hospital Essen.

Inflammation To determine the effect of inflammation, newborn rats were randomly assigned to the following groups (figure 2.1):

- 1: 0.1 ml/10 g NaCl 0.9% at P3
- 2: 0.25 mg/kg (0.1 ml/10 g) LPS at P3

Randomisation of rats was achieved determining the group by another person without knowing which rat has been picked. Animals were numbered with a marker (edding 3000) on their belly and numbers were renewed at least every two days. Weight was recorded at P3, P5, P6 and P11. Pups were decapitated on P6, P11 and at 2 h, 4 h, 8 h, 12 h and 24 h after administration of LPS. Gender was determined by inspection. Injections were carefully performed intraperitoneally with a syringe of 1 ml capacity with a 30 gauge needle by holding the rat head-down.

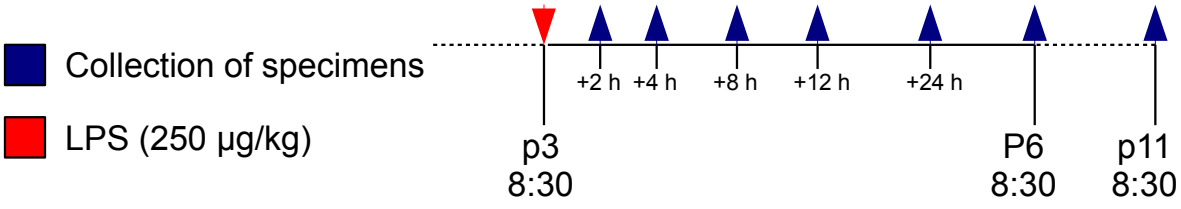

Figure 2.1.: **Protocol: Inflammation**

Recombinant human TSG-6 under inflammatory conditions To determine the effect of rhTSG-6 on newborn rats under inflammatory conditions, rats were randomly assigned to the following groups (figure 2.2):

- 1: 0.1 ml/10 g NaCl 0.9% at P3 and four repetitive doses of 0.15 ml/10 g PBS every 12 h, first dose 3 h before NaCl injection
- 2: 0.25 mg/kg (0.1 ml/10 g) LPS at P3 and four repetitive doses of 0.15 ml/10 g PBS every 12 h, first dose 3 h before LPS injection
- 3: 0.25 mg/kg (0.1 ml/10 g) LPS at P3 and four repetitive doses of 2.25 mg/kg (0.15 ml/10 g) rhTSG-6 every 12 h, first dose 3 h before LPS injection

Randomisation and administration of compounds was done as described above. Decapitation was performed on P3 + 6 h, P5 and P11. Whole brain hemispheres, cerebellum, heart, liver, lung, thymus, gut, spleen, skin and skeletal muscle from the thigh, whole blood and serum was collected. For this experimental project, only brain parts, serum and whole blood were further analysed.

2.2.1.1. Preparation of animals

Animals received an overdose of chloral hydrate (200 mg of chloral hydrate per kg body weight in 0.1 ml injection volume per 10 g body weight). After determining that the rat did not perceive any pain by giving a painful stimulus and observing its reaction, the skin and the underlying peritoneum were cut with a pair of scissors to open the abdomen. Rips were cut at both sides and diaphragma was severed to remove the anterior thorax. By cutting the left atrium, blood was collected using an EDTA-coated capillary tube in order to generate blood slides and perform blood counts, or absorbed with a pipette and centrifuged with 3000*g* at 4 °C to obtain serum as the supernatant. The spleen was removed and snap-frozen in liquid nitrogen prior to perfusion. Depending on the desired sample, perfusion with PBS and subsequent sterile 4% PFA in PBS was performed for histology or only with sterile PBS for RNA and protein investigations. Thereafter the retrieval of organs followed. Gut, liver, lung, heart and thymus were taken from the open abdomen and thorax. Skeletal muscle and skin samples were cut from the thighs. Brains were extracted by sagittally cutting the cranium and subsequent removal of the os occipitale and temporale. Afterwards the brain was removed with a spatula and cut into pieces as required (cerebellum + hemispheres/thalamus, cortex, striatum). Samples were stored for 48 h-72 h in 4% PFA in PBS at 4 °C and afterwards in

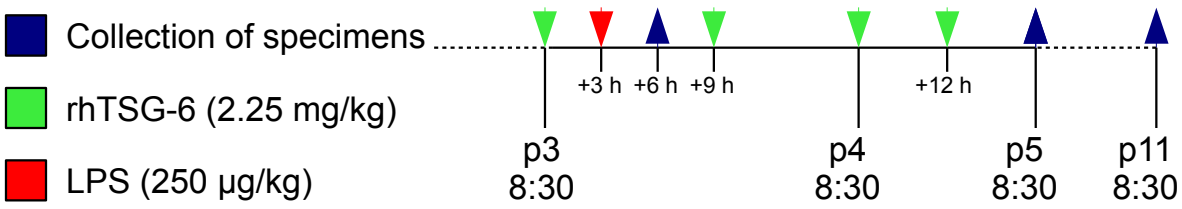

Figure 2.2.: **Protocol: Recombinant human TSG-6 under inflammatory conditions**

PBS at 4 °C for histology or snap-frozen in liquid nitrogen for RNA and protein investigations. Snap-frozen samples were stored for later use at -80 °C.

2.2.2. Real-time PCR

2.2.2.1. Extraction of RNA

Frozen samples were put into TRIzol® filled 15 ml conical centrifuge tubes and immediately crushed with a pipette until tissue was completely dissolved. The TRIzol®/tissue ratio was 1 ml per 75 mg. After incubating for 5 min, 0.2 ml chloroform per ml TRIzol® was added and the mix was vortexed until it was homogeneous. After further incubation for 3 min, the mix was evenly distributed among smaller reaction tubes and separated into three phases by centrifuging at 4 °C with 12.500*g* for 20 min. The upper aqueous phase was transferred into new tubes and an equivalent amount of isopropanol was added. After vortexing and 10 min of incubation, samples were centrifuged at 4 °C with 12.500*g* for 10 min. Supernatant was removed and each pellet diluted in 800 µl 75% ethanol, followed by another step of vortexing and centrifuging at 4 °C with 7500*g* for 5 min. Supernatants were again removed and pellets were dried in a dust-free environment for about 20 min. Dried pellets were diluted in 100-200 µl aqua ad iniectabilia while cycling in a thermomixer at 65 °C for 15 min. Quantity and quality was photometrically determined with a NanoDrop 1000 Spectrophotometer. Quantity was measured at 260 nm and quality by calculating the ratio of 260 nm/280 nm and 230 nm/260 nm. Samples were stored for further use at -80 °C.

2.2.2.2. Reverse Transcription of RNA

RNA was defrosted and diluted to a concentration of 250-1000 ng/µl depending on the initial concentration. Stripes of 8 PCR tubes were filled with DNAse Master Mix using a multipette and thereafter RNA was added. Stripes were centrifuged and incubated for 15 min. 1 µl EDTA was added and another step of centrifugation was performed. Stripes were incubated for 10 min in the preheated T3 Thermocycler at 65 °C and afterwards cooled down to 4 °C. In the meantime, further stripes were filled with RT Master Mix I. These stripes were filled with 5 µl of incubated DNAse Master Mix/RNA solution, centrifuged and incubated in the preheated T3 Thermocycler at 65 °C for 5 min. After incubation stripes were immediately cooled on ice and every further step was performed under cooled conditions. 10 µl RT Master Mix II was added to each well of RT Master Mix I/DNAse Master Mix/RNA solution and centrifuged. The RNA was converted to cDNA by using the T3 Thermocycler with the following heating steps: 5 min 25 °C $\rightarrow$ 60 min 42 °C $\rightarrow$ 10 min 70 °C $\rightarrow$ 4 °C. Then, the cDNA solution was diluted 1:1 with H_2O.

2.2.2.3. Real-time PCR

Relative quantification of gene expression was analysed using real-time PCR and the $2^{-\Delta\Delta C_T}$ method (Livak, Schmittgen, 2001). The cDNA solution was defrosted and a real-time PCR Master Mix (every component but cDNA) for each gene target was admixed (see Table 2.9).

Target	Ingredient	Volume
TSG-6	Forward/Reverse Primer [5 µM]	3 µl
	Probe [5 µM]	1 µl
	TaqMan® Fast Universal PCR Master Mix (2x)	10 µl
	H_2O	4 µl
	cDNA	2 µl
GAPDH	Forward/Reverse Primer [5 µM]	3 µl
	Probe [5 µM]	1 µl
	TaqMan® Fast Universal PCR Master Mix (2x)	10 µl
	H_2O	4 µl
	cDNA	2 µl
Ubiquitin	Forward/Reverse Primer [5 µM]	3 µl
	Probe [5 µM]	1 µl
	TaqMan® Fast Universal PCR Master Mix (2x)	10 µl
	H_2O	4 µl
	cDNA	2 µl

Table 2.9.: real-time PCR components

The cDNA was transferred to a 96-well plate. Afterwards PCR Master Mix was added by using a multipette and carefully pipetted at the well's wall in order to prevent contamination. The first well, in which PCR Master Mix was added, was a negative control containing H_2O. Measurements were performed as doublets. After preparing the 96-well plate, it was covered with MicroAmp® Optical Adhesive Film and put into a StepOne Plus machine. Denaturation was performed at 95 °C for one second, annealing and elongation followed at 60 °C for 20 seconds. These steps were cycled 40 times. The generated data was exported and evaluated. The maximum tolerance of standard deviation of the C_T value in each duplicate measurement was 0.5 as proposed by the StepOne Plus Software.

2.2.3. Immunoblotting

2.2.3.1. Protein extraction

First, a cell-lysis solution containing 1/7 cOmplete Mini and 1/100 PMSF dissolved in RIPA buffer was prepared. Frozen samples were transferred to labelled reaction tubes and cell-lysis solution was added (see Table 2.10). Samples were carefully crushed with a pipette until the solution was homogeneous. The nucleic fraction was separated by centrifuging at 4 °C with 3000*g* for 15 min. Afterwards supernatants were transferred to new tubes. To separate the mitochondrial fraction a further step of centrifugation at 4 °C with 17000*g* for 20 min followed. Supernatants were again transferred into new tubes and stored at -80 °C for later use. Protein concentration of isolated samples was determined by analysing the photometric absorption after Bicinchoninic acid assay (BCA) Cu^{2+} reaction and compared to a concentration series of solved BSA (five exponential steps from 1000 ng/µl to 62.5 ng/µl and H_2O as a negative control). Samples were diluted 1:10 using H_2O. Standards were measured as doublets. First, 10 µl of standard or sample was transferred to a 96-well plate and afterwards 150 µl of BCA® protein assay was added to each well. The plate was covered with its lid and incubated

Tissue	Volume
Hemisphere P1	300 µl
Hemisphere P3	300 µl
Hemisphere P5	600 µl
Hemisphere P7	600 µl
Hemisphere P9	900 µl
Hemisphere P11	900 µl
Hemisphere P13	1200 µl
Hemisphere P15	1200 µl

Table 2.10.: Amount of cell-lysis solution for different tissue

at 37 °C for 30 min. Thereafter the photometric absorption was determined by an Infinite M200. Protein concentrations of samples were determined by calculating a simple linear regression model, which relates the protein concentration to the photometric absorption of the concentration series. The samples were stored for further use at -80 °C.

2.2.3.2. Polyacrylamid Gelelectrophoresis

Extracted proteins were first diluted to 6 µg/µl and mixed with an equivalent amount of Laemmli buffer. After incubation at 95 °C for 10 min in a preheated thermomixer, samples were stored at -20 °C or directly used for further analysis. Gelelectrophoresis was performed on Maxigel. It consists of a stand with a lower and an upper pool, its lid and two pairs of glass plates. The glass plates were cleaned with ethanol and each pair was combined to create a mould which was sealed with silicone rubber at the outer sides. After attaching the mould to the stand, it was filled with separating gel to about 70% capacity and the liquid level was straightened with 250 µl isopropanol. After the separating gel was hardened, isopropanol was washed out with H_2O and the mould was dried with blotting paper. Then, the rest of the mould was filled with stacking gel and formed to slots by a comb. After hardening of the stacking gel, the pools of Maxigel were filled with electrophoresis buffer, the comb was removed and slots were cleaned with a 100 µl Hamilton-Pipette using electrophoresis buffer. Each slot was filled with 10 µl of sample and one slot was filled with Precision Plus Protein Standards Dual Color for later identification of the molecular weight of proteins. Thereafter, the stand was closed with its lid and voltage of 80 V was attached. When the dye front reached the separating gel, voltage was elevated to 150 V.

2.2.3.3. Immunoblotting

Shortly before the dye front reached the end of the separating gel, voltage was detached and the separating gel was transferred to a Criterion Blotter Gel Holder Cassette with a red (anode) and a black (cathode) side. From anode to cathode the cassette was filled with: foam pad $\rightarrow$ blotting paper $\rightarrow$ nitrocellulose membrane (Amersham Protran) $\rightarrow$ separating gel containing the samples $\rightarrow$ blotting paper $\rightarrow$ foam pad. The cassette was transferred to a Criterion Blotter Buffer Tank, which was then filled with precooled transfer buffer and voltage of 100 V was attached for 75 min. Thereafter the cage was removed and the nitrocellulose

pri. Antibody	conc.	sec. Antibody	conc.	blocking buffer
anti-TSG-6 (AF2104)	1/80	anti-goat HRP	1/5000	WB
anti-Iba1	1/1000	anti-rabbit HRP	1/1000	MP
anti-cleaved-caspase-3	1/1000	anti-rabbit HRP	1/1000	MP
anti-β-actin	1/1000	anti-rabbit HRP	1/1000	MP
anti-GAPDH	1/1000	anti-rabbit HRP	1/2000	MP

Table 2.11.: Antibodies used in Western Blotting

membrane was washed in TBS-T for 3 x 5 min. For rapid reversible detection of protein bands the nitrocellulose membrane was incubated in Ponceau S solution. The membrane was labelled and regions without protein were cut off. After further washing in TBS-T for 3 x 5 min, the nitrocellulose membrane was incubated in blocking solution (table 2.11) for 1 hour and then incubated in primary antibody/blocking solution mix at 4 °C over night. The next day, the nitrocellulose membrane was washed in TBS-T for 3 x 5 min and incubated in secondary antibody solution for 60 min.

2.2.3.4. Densitometric quantification of protein expression

The nitrocellulose membrane was washed in TBS-T for 3 x 5 min, incubated in Amersham ECL Plus reagent for 5 min in the dark and analysed by a Bio-Rad ChemiDoc XRS+ System using chemiluminescence imaging. The exposure time differed with a maximum of 20 min. Data generated by the ChemiDoc was further processed by the included software Image Lab to generate an image with the chemiluminescence intensity encoded as grey tones displaying clustered protein bands. Appropriate protein bands were identified by comparing the molecular weight of the target protein with the Precision Plus Protein Standards Dual Color bands. Single bands were selected and the integral of the chemiluminescence intensity was calculated. Finally, a spreadsheet containing the densitometrically quantified protein expression was exported.

2.2.3.5. Quantification of β-actin/GAPDH as a reference protein

After the target protein was analysed, the nitrocellulose membrane was washed in TBS-T for 3 x 5 min and a further step of incubation with anti-β-actin/GAPDH followed as described in 2.2.3.3, but with primary antibody incubation of one hour at room temperature. Analysis was as described in 2.2.3.4.

2.2.4. Multiplex ELISA analysis

Multiplex ELISA analysis was performed using a Luminex 200 device with Bio-Plex Pro Rat Cytokine Assays.

2.2.4.1. Preparation of liquids

All liquids were prepared shortly before use during assay preparation.

Standards The lyophilized standard was diluted in 500 µl standard diluent, gently vortexed and incubated on ice for 30 min. An eight-point standard curve with a fourfold dilution between each point was prepared from the reconstituted standard. Nine 1.5 ml tubes were labelled S1 to S8 and Blank. The S1 tube was filled with 72 ml standard diluent, 128 ml reconstituted standard and gently vortexed. Tubes were filled with 150 ml standard diluent, 50 ml of the next higher concentration and vortexed. The Blank tube was filled with 150 ml standard diluent.

Samples Serum was diluted 1:4 by adding sample diluent. Brain hemispheres from P3 were prepared using Bio-Plex® Cell Lysis Kit. Each sample was incubated in 600 µl lysis solution, containing 240 µl Factor 1, 120 µl Factor 2 and 240 µl 500 mM PMSF. Brain hemispheres were then crushed with a pipette. Protein concentration was determined according to 2.2.3.2. Finally tissue samples were diluted to a concentration of 900 µg/ml using sample diluent.

Coupled beads The coupled beads had a stock concentration of 20x. They were diluted 1:20 in assay buffer and gently vortexed.

Detection antibodies The detection antibodies had a stock concentration of 20x. They were diluted 1:20 in assay buffer and gently vortexed.

Streptavidin Phycoerythrin The SA-PE had a stock concentration of 100x. They were diluted 1:100 in assay buffer, gently vortexed and protected from light until use.

Washing The 96-well plate was washed using a Bio-Plex Handheld Magnetic Washer. The plate was attached to the washer and incubated for 1 min to make sure that the magnetic beads were held in place by the magnet of the washer. The plate was held upside-down to remove all liquid and gently tapped on a paper towel to remove any excess liquid. The plate was detached from the washer, each well was filled with 100 µl of washing buffer and after 1 min of incubation, the plate was again attached to the washer and cleared from any liquid.

2.2.4.2. Preparation of the Luminex 200

The plate layout was designed using the IS2.3 or Xponent 3.1 software by Luminex. RP1 (PMT) was set to high, DD gates were set to 5,000-25,000 and Bead events to 50. The Luminex 200 was calibrated before use.

2.2.4.3. Preparation of the Multiplex ELISA assay

The assay was admixed in a 96-well plate. First, 50 µl of prepared coupled beads was transferred to each well. After washing two times, 50 µl of prepared standard or sample, respectively, was transferred to each well. The plate was covered and protected from light with sealing tape and incubated on a shaker at 850 rpm at room temperature for 60 min. After removing the tape and washing three times, 25 µl of prepared detection antibodies was transferred to each well. The plate was again covered and protected from light with sealing

tape and incubated on a shaker at 850 rpm at room temperature for 30 min. After removing the tape and washing three times, 50 µl of prepared SA-PE was transferred to each well. The plate was once more covered and protected from light with sealing tape and incubated on a shaker at 850 rpm at room temperature for 10 min. After removing the tape and washing three times, 125 µl of assay buffer was transferred to each well. The plate was covered and protected from light with sealing tape and incubated on a shaker at 850 rpm at room temperature for 30 sec. After removing the tape, the plate could finally be analysed by a Luminex 200 device.

2.2.4.4. Evaluation of data

The generated data was exported as .csv files and evaluated using the nCal package (Fong, Sebestyen, 2013; Ritz, Streibig, 2005) for R statistical environment.

2.2.5. Blood analysis

2.2.5.1. Blood count

50 µl freshly obtained blood from Wistar rats was transferred to tubes filled with 200 µl EDTA and analysed by the central laboratory of the University Hospital Essen.

2.2.5.2. Differential blood count

A drop of freshly obtained blood from Wistar rats was transferred to a slide and slowly smeared with the edge of a second slide, creating a thin, even coating. After drying, the slides were stained with Pappenheim's stain. They were first incubated in May-Grünwald's eosin methylene blue for 5 min and afterwards washed four times in tap water for 5 min. A giemsa solution was prepared containing 12 ml filtered Giemsa's azur-eosin-methylene blue and 180 ml of buffered H_2O (one Buffer tablet pH 6.8 in 1 l H_2O). The slides were incubated in giemsa solution for 20 min and again washed four times in tap water for 5 min. Blood smears were evaluated by the Peadiatric Oncology laboratory of the University Hospital Essen.

2.2.6. Histology and immunohistochemistry

2.2.6.1. Tissue fixation in paraffin blocks

PFA-fixed tissue was transferred to paraffin according to standard protocols by the Department of Pathology of the University Hospital Essen. Afterwards, specimens were embedded in paraffin blocks and attached to embedding cassettes, using a TES99. Brain hemispheres were rotated that the coronal plane was orientated horizontally, resulting in coronary sections after microdissection.

2.2.6.2. Microdissection of paraffin blocks into ultra-thin slices

The paraffin blocks were attached to a Microm HM 430 and cut into 10 µm thin slices, which were grouped in sections of four sequent slices. The sections were carefully transferred with

a brush to an about 60 °C warm water bath (HIR-3). After the slices were smoothened in the water bath, every fifth section was transferred to previously labelled standard slides for HE staining. The other sections were transferred to previously labelled SuperFrost® Plus slides for immunohistochemical staining.

2.2.6.3. Staining of ultra-thin slices

Every staining started with the deparaffinisation and rehydration of the slices. This was achieved by incubation of the slides in glass staining dishes filled with the following liquids. Xylene 2 x 10 min $\rightarrow$ 100% ethanol 2 x 5 min $\rightarrow$ 96% ethanol 1 x 5 min $\rightarrow$ 70% ethanol 1 x 5 min $\rightarrow$ 50% ethanol 1 x 5 min $\rightarrow$ H_2O 1 x 2 min.

HE staining Hematoxylin and eosin staining was performed by the Department of Pathology of the University Hospital Essen according to standard protocols.

Immunohistological staining Immunohistological staining started with antigen retrieval. The slides, stored in cuvettes, were incubated in citrate buffer and heated in a microwave until boiling with 700 W and afterwards heated at 150 W for 10 min. Then, the slides were cooled down for at least 30 min. Afterwards, the slides where attached to coverplates for the following incubation steps. The detailed fluids used are described in table 2.12. The slides were rinsed three times in 1 ml TBS-T for 5 min. The following step was only applied on DAB staining: 20 min incubation in the dark in H_2O_2/methanol solution and rinsing three times in 1 ml TBS-T for 5 min. 150 µl blocking solution was added for 45 min. Over night, the slides were incubated in 100 µl primary antibody in blocking solution at 4 °C. The next day, the slides were either prepared for fluorescence staining or DAB staining.

Fluorescence For fluorescence staining, the slides were rinsed three times in 1 ml TBS-T for 5 min and 100 µl secondary antibody in TBS-T was added for 45 min. For staining of cell nuclei, 100 µl PBS-DAPI (100 ng/ml) was added for 5 min. Then, the slides were again rinsed three times in 1 ml PBS for 5 min, removed from the coverplates, stored in glass staining dishes and washed in H_2O three times for 5 min. Finally, the slides were carefully covered with coverslips, using Fluorescence Mounting Medium, labelled and stored for later use.

DAB For DAB staining, the slides were rinsed three times in 1 ml TBS-T for 5 min and 100 µl secondary antibody in TBS-T was added for 120 min. Thereafter, the slides were rinsed three times in 1 ml PBS for 5 min. 100 µl ABC solution was added for 60 min. Then, the slides were rinsed two times in PBS for 5 min and once in TBS for 5 min. 400 µl DAB solution was added for 6 min and afterwards 1 ml of cold H_2O was applied to stop the staining. Counterstaining was performed by applying nuclear fast red solution for 20 s and washing with 1 ml cold H_2O. After rinsing three times in TBS for 5 min, the slides were removed from the coverplates and stored in glass staining dishes. Dehydration was performed by the following incubation steps: H_2O 1 x 2 min $\rightarrow$ 50% ethanol 1 x 5 min $\rightarrow$ 70% ethanol 1 x 5 min $\rightarrow$ 96%

pri. Antibody	conc.	sec. Antibody	conc.	buffer	type
anti-TSG-6 (FL-277)	1/25	anti-rabbit 594	1/500	IHC	fluorescence
anti-TSG-6 (E-10)	1/25	anti-mouse 594	1/500	IHC	fluorescence
anti-TSG-6 (AF2104)	1/10	anti-goat 594	1/500	IHC	fluorescence
anti-TSG-6 (FL-277)	1/25	anti-rabbit biotinylated	1/500	IHC	DAB
anti-TSG-6 (E-10)	1/25	anti-mouse biotinylated	1/500	IHC	DAB
anti-TSG-6 (AF2104)	1/10	anti-goat biotinylated	1/500	IHC	DAB

Table 2.12.: Antibodies used for IHC

ethanol 1 x 5 min $\rightarrow$ 100% ethanol 2 x 5 min $\rightarrow$ Xylene 2 x 10 min. Finally, the slides were carefully covered with coverslips, using Eukitt®, labelled and stored for later use.

2.2.6.4. Microscopic evaluation of stained tissue

The stained slides were evaluated using an Axioplan microscope with object lens magnifications from 10x to 40x in a dark room. Fluorescence was stimulated using a Colibri.2 light source. Images were taken with an AxioCam ICc1 for documentation.

2.2.7. Statistical analysis and graphical presentation

Statistical computing was done using R statistical environment (Team, R Core Team, 2012) and the dedicated integrated development environment RStudio. Additional packages used were gdata (Warnes et al., 2012), ggplot2 (Wickham, 2009), stringr (Wickham, 2012) and nCal (Fong, Sebestyen, 2013; Ritz, Streibig, 2005). Most data were $\log_2$ transformed to improve standard distribution of data. p-Values were calculated using analysis of variance models fitted into Tukey's Honest Significant Difference' method as well as pairwise t-test using the Holm-Bonferroni method for multiple testing (#: $p > 0.05$, $*$: $p < 0.05$, $**$: $p < 0.01$, $***$: $p < 0.001$). Graphical presentation was generated using ggplot2.

3. Results

3.1. Staining

For TSG-6 IHC staining we tested multiple antibodies and fluorescence/DAB staining. Tissue tested was brain, skin and skeletal muscle, which was reported to express large amounts of TSG-6 mRNA (Milner, Day, 2003). However, we did not achieve a convincing staining of TSG-6. Formalin-fixed paraffin-embedded (FFPE) tissue is reliant on antigen retrieval to reveal epitopes for antibodies. Heating is the most favorite kind of antigen retrieval, but it is not guaranteed that all epitopes retain their full structure (Shi et al., 2011). Cryo embedding is an alternative to FFPE which remains to be tested.

3.2. Developmental regulation of TSG-6 in the neonatal brain

We detected TSG-6 in the healthy neonatal rat brain at both mRNA and protein level by real-time PCR and Western blotting (figure 3.1). At the mRNA level, TSG-6 expression increased constantly from P1 to P15, at P15 TSG-6 expression was 3-fold higher than at P1. Calculating linear regression revealed a strong association between TSG-6 mRNA expression and day of life (coefficient of determination = 0.9675). At the protein level, TSG-6 expression showed high statistical variability and only weak association with the day of life (coefficient of determination = 0.15). TSG-6 expression in selected brain regions (hemispheres, cortex, thalamus, striatum) on P6 revealed significant differences between the regions. The pattern of local TSG-6 expression was similar at mRNA and protein level, although differences in mRNA levels were larger (figure 3.2). In the cortex, expression was lower than in whole hemispheres with -17% at protein level and -12% at the mRNA level. Lower expression was also detected in the thalamus showing -30% at protein level and -63% at the mRNA level. Striatum showed ambivalent expression with +9% at protein level and -45% at the mRNA level. All differences between mRNA expression in any brain region were statistically significant (table 3.1), while only the differences between TSG-6 protein expression in thalamus and in hemispheres/striatum reached statistical significance (table 3.2).

3.3. Immune response after inflammatory stimulus in the neonatal rat

Administration of LPS to newborn Wistar pups at P3 induced an extensive, systemic inflammatory response (figure 3.3), including up-regulation of pro-inflammatory cytokines, anti-inflammatory cytokines and chemokines. The immune response peaked between 2 and

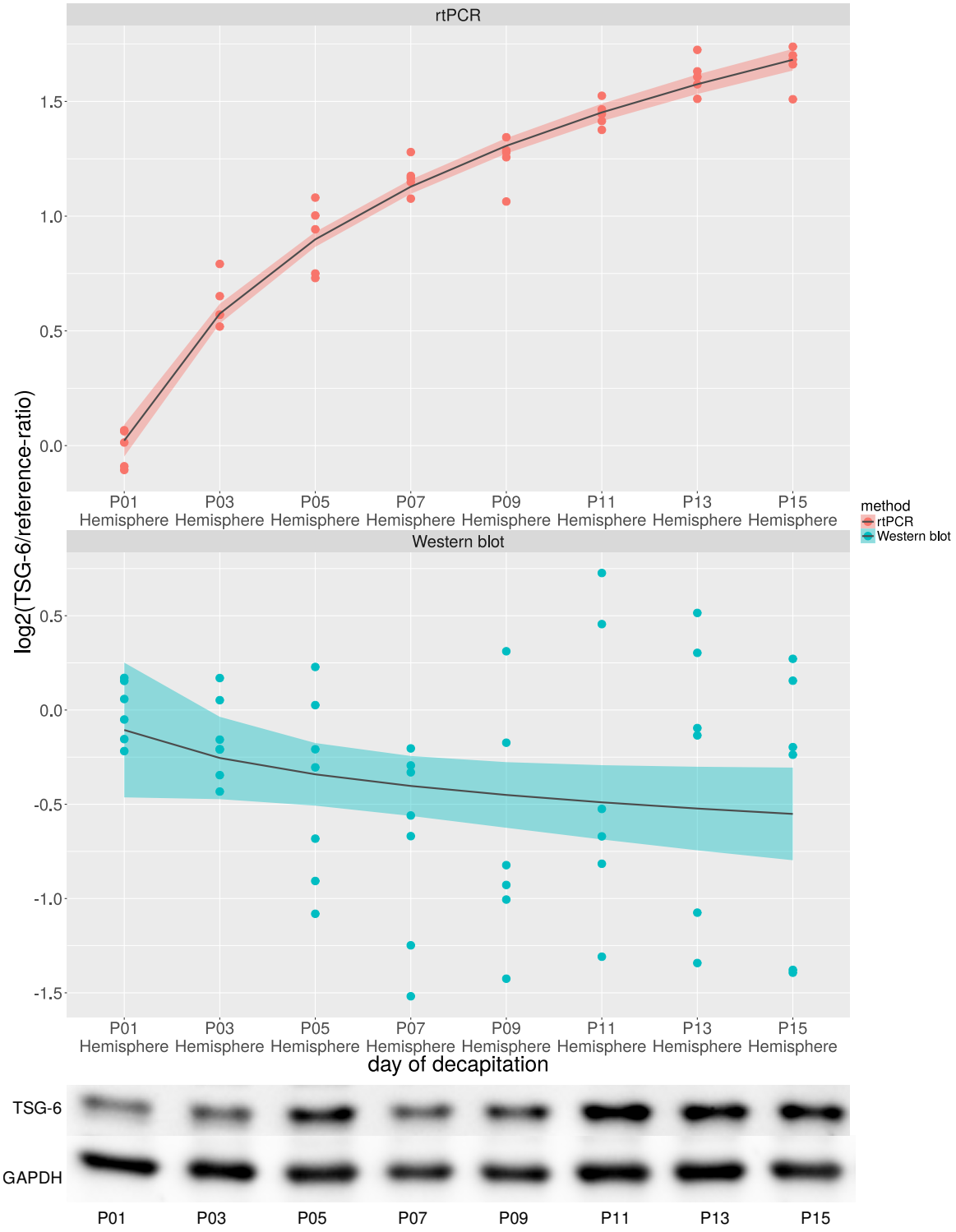

Figure 3.1.: **Developmental expression of TSG-6 in newborn rat brains**
TSG-6 mRNA is linearly up-regulated from P1 to P15 by about 3-fold. TSG-6 protein shows high statistical spreading, but it is certainly expressed in the neonatal rat brain.
Method: rtPCR (reference: Ubiquitin)/Western blot (reference: GAPDH), *samples:* hemispheres/n = 4-7, *treatment:* decapitation 1-15 days after birth (P1-P15), *graphics:* points $\pm$ CI, *statistics:* linear regression ($y = log2(x)$)/coefficient of determination = 0.9675 (rtPCR)/0.15 (Western blot).

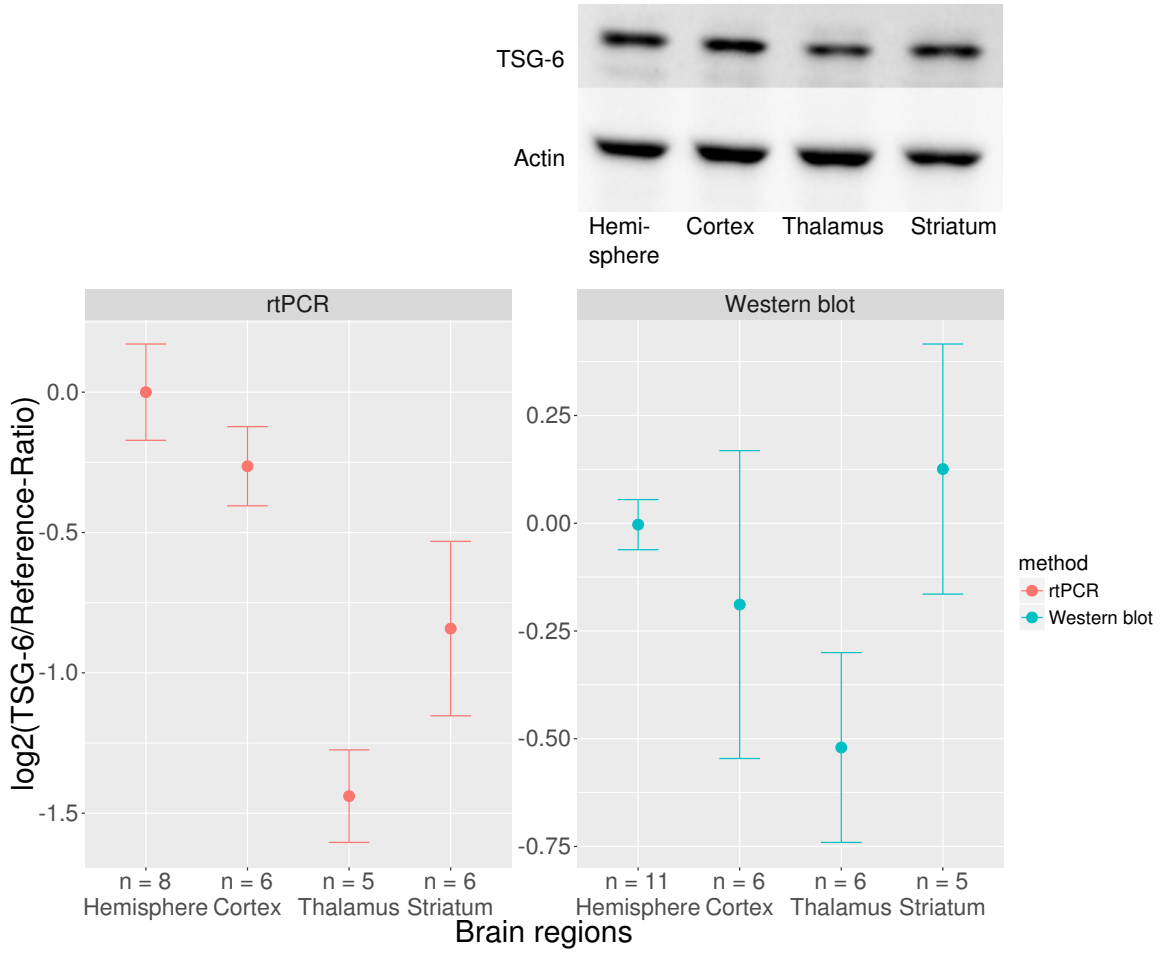

Figure 3.2.: **Expression of TSG-6 mRNA/protein in different brain regions**
TSG-6 mRNA and protein expression varies between different brain regions. It is lower in thalamus, cortex and striatum than in whole hemispheres with the exception of striatum at protein level.
Method: rtPCR (reference: GAPDH)/Western blot (reference: β-actin), *samples:* brain regions/n = 5-11, *treatment:* injection of sodium chloride 0.9% on P3/decapitation on P6, *graphics:* error plots ± CI, *statistics:* pairwise t-test/p-values displayed in table 3.1 and 3.2

Table 3.1.: p-Values of TSG-6 mRNA expression in different brain regions

	Cortex	Hemisphere	Striatum
Hemisphere	0.027 56	-	-
Striatum	0.000 25	8.1×10^{-7}	-
Thalamus	2.8×10^{-8}	3.0×10^{-10}	0.000 25

Table 3.2.: p-Values of TSG-6 protein expression in different brain regions

	Cortex	Hemisphere	Striatum
Hemisphere	0.199 32	-	-
Striatum	0.068 28	0.273 50	-
Thalamus	0.050 96	0.000 37	0.000 25

8 h after i.p. LPS administration. Interestingly, after 48 h (figure 3.4), the immune response reversed to lower levels than in sham-treated animals, with serum Interferon-γ and IL-6 being reduced the most to levels of less than 30% of the controls. Additionally, under inflammatory conditions, the proportion of lymphocytes in the differential blood count was decreased by 10% from 76% to 68%, while the proportion of monocytes was elevated by 60% from 10% to 16% (figure 3.6). The amount of thrombocytes also decreased by 58% from 350 k to 150 k (figure 3.5). In the brain, cytokine levels were below the detection limit (data not shown).

3.4. Regulation of TSG-6 under inflammatory conditions in the neonatal brain

As TSG-6, known for pronounced anti-inflammatory activities, is expressed in the developing brain, we investigated whether TSG-6 levels in the brain were altered after i.p. LPS administration. Figure 3.7 shows the TSG-6 expression 0-24 h after LPS stimulus on P3. At the mRNA level, TSG-6 expression in the brain was significantly up-regulated after LPS exposure. The maximum expression was reached 4 h after LPS administration with +52% and returned to normal levels after 12 h. At the protein level, statistical variability was higher than at the mRNA level and no significant differences in expression levels were detected. Later time-points (P6+P11 for hemisphere, P6 for brain regions) did not exhibit significant differences of TSG-6 expression in hemispheres, cortex, thalamus and striatum at the mRNA and protein level between LPS and sham-treated animals (figure 3.8, figure 3.9, figure 3.10).

3.5. Systemic and local effects of repetitive TSG-6 application on neonatal rats after inflammatory stimulus

Pups which received LPS on P3 and TSG-6 on P3 + P4 were evaluated on P5 for cleaved caspase-3 and microglia activation in the brain. Cytokine levels and cell counts in blood were investigated on P3 and P5. Figure 3.11 shows the presence of cleaved caspase-3 in the different treatment groups. LPS exposure increased levels of cleaved caspase-3 by 3-fold, but additional TSG-6 administration decreased this up-regulation by about 30%. The same samples were evaluated for Iba1 (figure 3.12), a marker for activated microglia (Boche et al., 2013). Its expression was significantly up-regulated by about 50% after LPS and remained elevated after additional treatment with TSG-6. Figure 3.13 shows the expression of selected cytokines in serum in the different treatment groups 6 h after inflammatory stimulus. Interferon-γ, IL-1β and MIP-3α were highly up-regulated by LPS treatment, but down-regulated by additional TSG-6 treatment (Interferon-γ: back to initial value, IL-1β: down-regulated by 25%, MIP-3α: down-regulated by 70%). Figure 3.4 shows the expression of selected cytokines in serum in the different treatment groups on P5. The down-regulation of cytokines by LPS was not affected by TSG-6, with the exception of IL-18, whose decrease was amplified by 36% from 0.29 pg/µl to 0.23 pg/µl. Cell counts in blood after inflammatory stimulus were not affected by TSG-6, either (figure 3.5, figure 3.6).

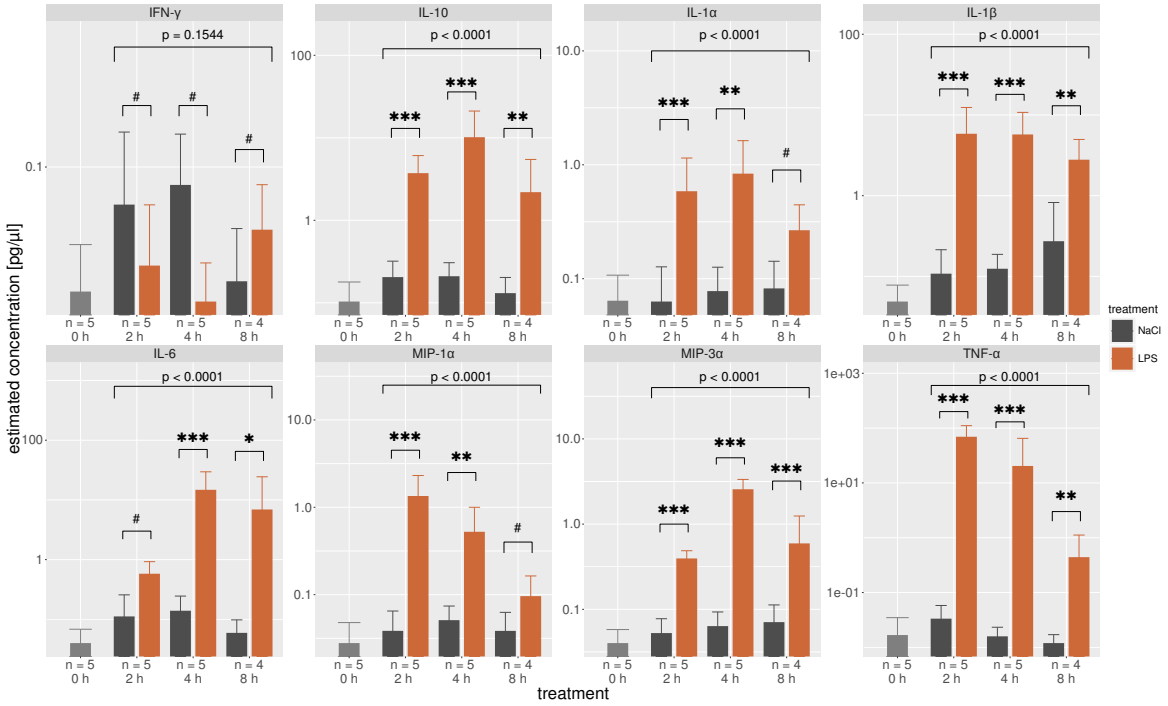

Figure 3.3.: **Systemic inflammatory response in the first 8 h after inflammatory stimulus**
Cytokine expression is elevated in serum 2-8 h after LPS-induced inflammation indicating a massive systemic response.
Method: multiplex ELISA, *samples:* serum/n = 4-5, *treatment:* NaCl = sodium chloride 0.9% [P3]/LPS = lipopolysaccharide 0.25 mg/kg [P3]/decapitation on P3 + 0-8 h, *graphics:* bar plots + CI, *statistics:* Tukey's honest significance test (#: $p > 0.05$, $*$: $p < 0.05$, $**$: $p < 0.01$, $***$: $p < 0.001$).

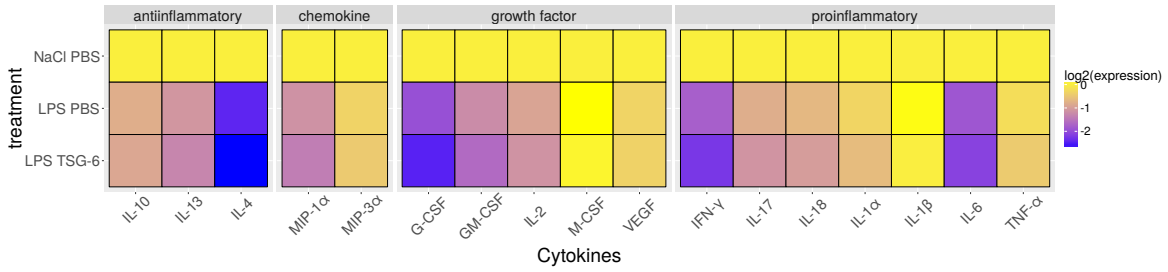

Figure 3.4.: **Systemic inflammatory response 48 h after inflammatory stimulus**
Cytokine expression is decreased in serum 48 h after inflammatory stimulus. This could contribute to the preconditioning effect of LPS on second insults. Additional TSG-6 treatment slightly amplifies the decrease.
Method: multiplex ELISA, *samples:* serum/n = 12-15, *treatment:* NaCl = sodium chloride 0.9% [P3]/LPS = lipopolysaccharide 0.25 mg/kg [P3]/TSG-6 = TSG-6 2.25 mg/kg 2x/d [P3+P4]/PBS = phosphate buffered saline 2x/d [P3+P4]/decapitation on P5, *graphics:* bar plots + CI, *statistics:* pairwise t-test/p-Values displayed in table 3.3

Table 3.3.: p-Values of systemic inflammatory response 48 h after inflammatory stimulus and TSG-6 treatment

G-CSF

	NaCl PBS	LPS PBS
LPS PBS	0.000 49	-
LPS TSG-6	1.6×10^{-5}	0.201 72

GM-CSF

	NaCl PBS	LPS PBS
LPS PBS	0.000 57	-
LPS TSG-6	9.7×10^{-6}	0.140 88

IFN-γ

	NaCl PBS	LPS PBS
LPS PBS	0.000 85	-
LPS TSG-6	1.2×10^{-5}	0.126 16

IL-10

	NaCl PBS	LPS PBS
LPS PBS	0.0064	-
LPS TSG-6	0.0032	0.6497

IL-13

	NaCl PBS	LPS PBS
LPS PBS	0.000 12	-
LPS TSG-6	1.3×10^{-5}	0.361 34

IL-17

	NaCl PBS	LPS PBS
LPS PBS	6.3×10^{-5}	-
LPS TSG-6	6.2×10^{-7}	0.11

IL-18

	NaCl PBS	LPS PBS
LPS PBS	0.000 11	-
LPS TSG-6	2.6×10^{-7}	0.040 12

IL-1α

	NaCl PBS	LPS PBS
LPS PBS	0.47	-
LPS TSG-6	0.09	0.47

IL-1β

	NaCl PBS	LPS PBS
LPS PBS	0.78	-
LPS TSG-6	0.89	0.89

IL-2

	NaCl PBS	LPS PBS
LPS PBS	7.8×10^{-6}	-
LPS TSG-6	1.8×10^{-7}	0.16

IL-4

	NaCl PBS	LPS PBS
LPS PBS	9.6×10^{-6}	-
LPS TSG-6	3.5×10^{-6}	0.58

IL-6

	NaCl PBS	LPS PBS
LPS PBS	1.2×10^{-5}	-
LPS TSG-6	4.1×10^{-6}	0.57

M-CSF

	NaCl PBS	LPS PBS
LPS PBS	0.44	-
LPS TSG-6	0.86	0.86

MIP-1α

	NaCl PBS	LPS PBS
LPS PBS	7.2×10^{-5}	-
LPS TSG-6	5.1×10^{-6}	0.3

MIP-3α

	NaCl PBS	LPS PBS
LPS PBS	0.0460	-
LPS TSG-6	0.0081	0.3924

TNF-α

	NaCl PBS	LPS PBS
LPS PBS	0.173	-
LPS TSG-6	0.018	0.252

VEGF

	NaCl PBS	LPS PBS
LPS PBS	0.0153	-
LPS TSG-6	0.0077	0.6492

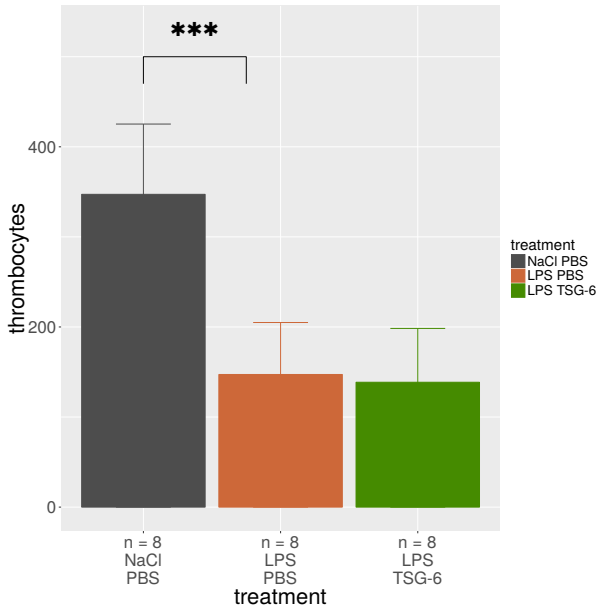

Figure 3.5.: **Thrombocytes 48 h after inflammatory stimulus**
Thrombocyte count is decreased under inflammatory conditions
Method: blood count, *samples:* blood/n = 8, *treatment:* NaCl = sodium chloride 0.9% [P3]/LPS = lipopolysaccharide 0.25 mg/kg [P3]/TSG-6 = TSG-6 2.25 mg/kg 2x/d [P3+P4]/PBS = phosphate buffered saline 2x/d [P3+P4]/decapitation on P5, *graphics:* bar plots + CI, *statistics:* pairwise t-test ($***$: $p < 0.001$)

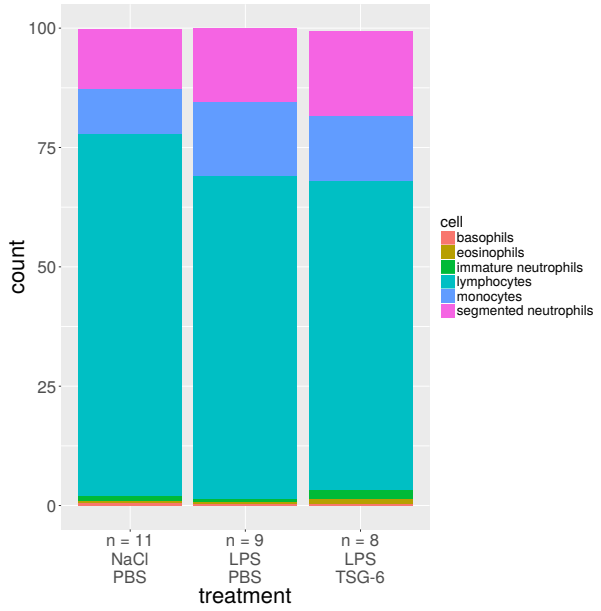

Figure 3.6.: **Systemic immune cell response 48 h after inflammatory stimulus**
Monocyte count in blood is increased under inflammatory conditions while lymphocyte count is decreased.
Method: differential blood count, *samples:* blood/n = 8-11, *treatment:* NaCl = sodium chloride 0.9% [P3]/LPS = lipopolysaccharide 0.25 mg/kg [P3]/TSG-6 = TSG-6 2.25 mg/kg 2x/d [P3+P4]/PBS = phosphate buffered saline 2x/d [P3+P4]/decapitation on P5, *graphics:* stacked bar plots, *statistics:* pairwise t-test/p-Values < 0.05 displayed in table 3.4

Table 3.4.: p-Values of systemic immune cell expression after inflammatory stimulus and TSG-6 treatment

	lymphocytes			monocytes	
	NaCl PBS	LPS PBS		NaCl PBS	LPS PBS
LPS PBS	0.0237	-	LPS PBS	0.033	-
LPS TSG-6	0.0042	0.3668	LPS TSG-6	0.155	0.440

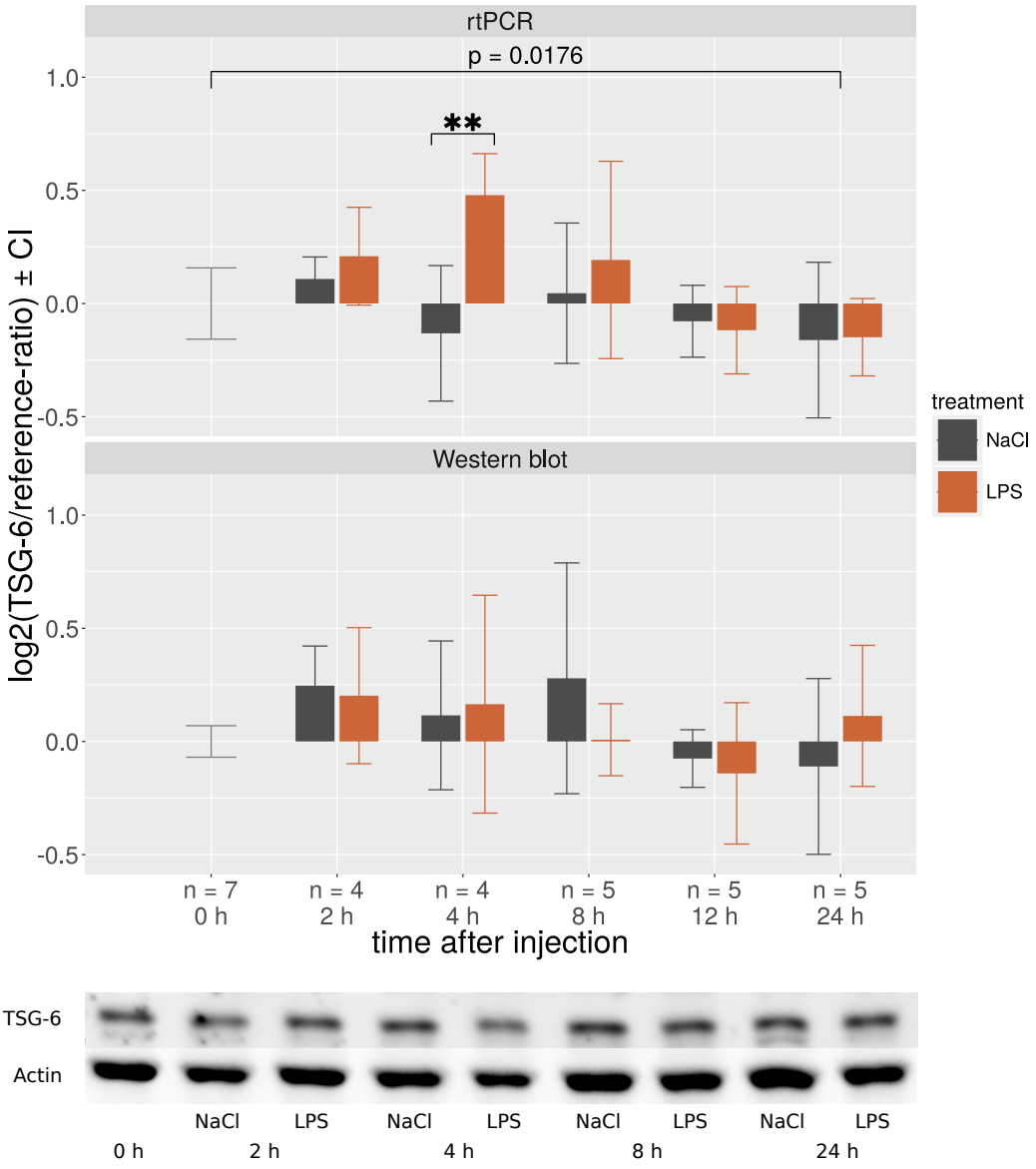

Figure 3.7.: **Expression of TSG-6 in brain hemispheres 0-24 h after inflammatory stimulus**
TSG-6 RNA expression in brain hemispheres is increased 4 h after LPS injection and therefore matching the peak of the systemic inflammatory response. TSG-6 protein expression in brain hemispheres is not altered 4 h after LPS injection. *Method:* rtPCR (reference: GAPDH)/Western blot (reference: β-actin), *samples:* hemispheres/n = 4-7, *treatment:* NaCl = sodium chloride 0.9% [P3]/LPS = lipopolysaccharide 0.25 mg/kg [P3]/decapitation on P3+0-24 h , *graphics:* bar plots ± CI, *statistics:* Tukey's honest significance test (**: $p < 0.01$).

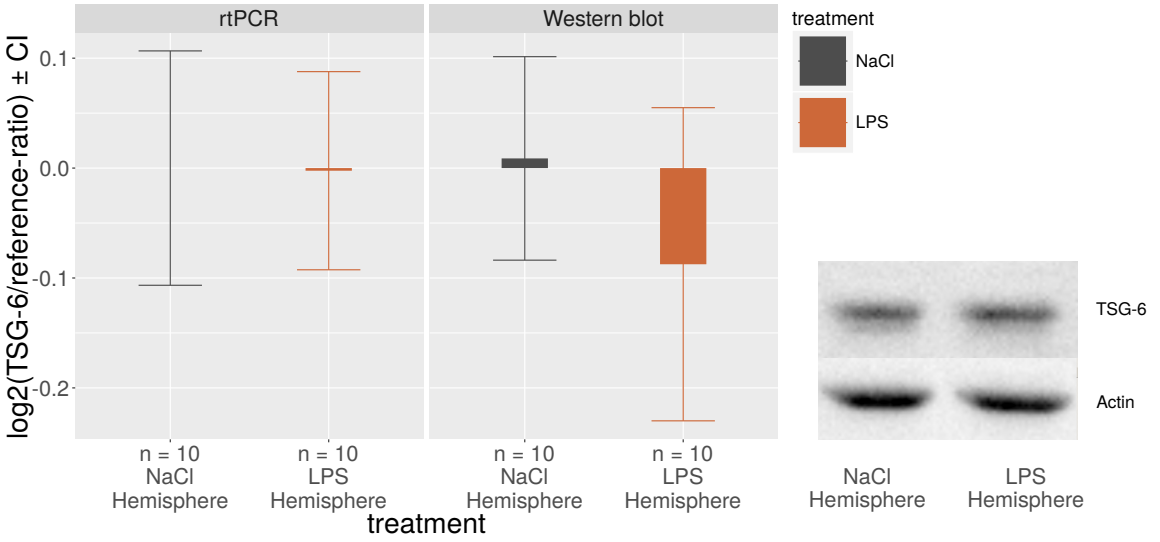

Figure 3.8.: **Expression of TSG-6 in brain hemispheres 3 days after inflammatory stimulus**
TSG-6 RNA/protein expression in brain hemispheres is not altered 3 days after LPS injection.
Method: rtPCR (reference: GAPDH)/Western blot (reference: β-actin), *samples:* hemispheres/n = 10, *treatment:* NaCl = sodium chloride 0.9% [P3]/LPS = lipopolysaccharide 0.25 mg/kg [P3]/decapitation on P6 , *graphics:* bar plots ± CI.

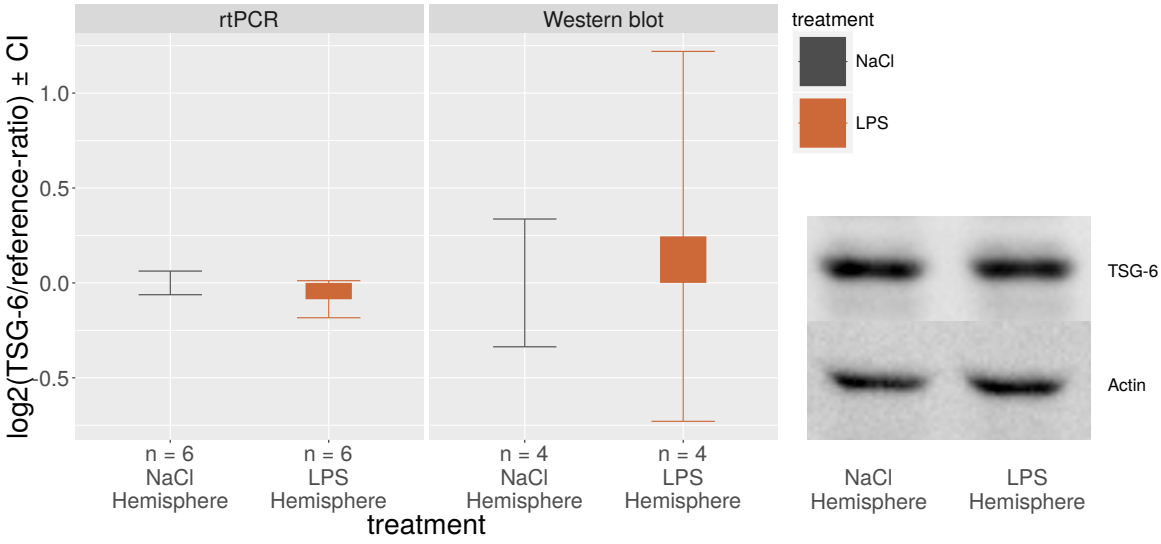

Figure 3.9.: **Expression of TSG-6 in brain hemispheres 8 days after inflammatory stimulus**
TSG-6 RNA/protein expression in brain hemispheres is not altered 8 days after LPS injection.
Method: rtPCR (reference: GAPDH)/Western blot (reference: β-actin), *samples:* hemispheres/n = 4-6, *treatment:* NaCl = sodium chloride 0.9% [P3]/LPS = lipopolysaccharide 0.25 mg/kg [P3]/decapitation on P11 h , *graphics:* bar plots ± CI.

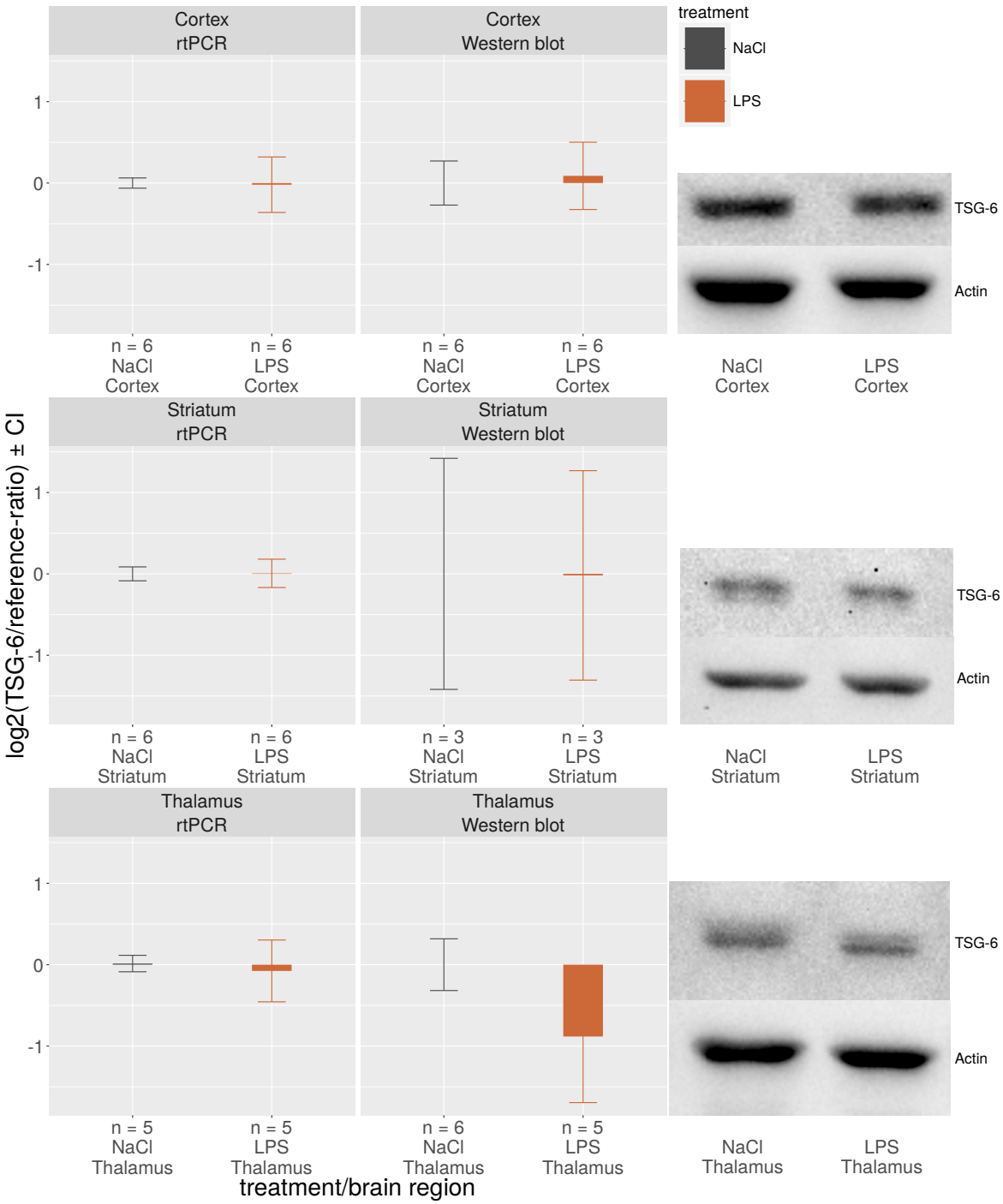

Figure 3.10.: **Expression of TSG-6 in different brain regions 3 days after inflammatory stimulus**
TSG-6 RNA/protein expression in different brain regions is not altered 3 days after LPS injection.
Method: rtPCR (reference: GAPDH)/Western blot (reference: β-actin), *samples:* brain regions/n = 3-6, *treatment:* NaCl = sodium chloride 0.9% [P3]/LPS = lipopolysaccharide 0.25 mg/kg [P3]/decapitation on P6 , *graphics:* bar plots ± CI.

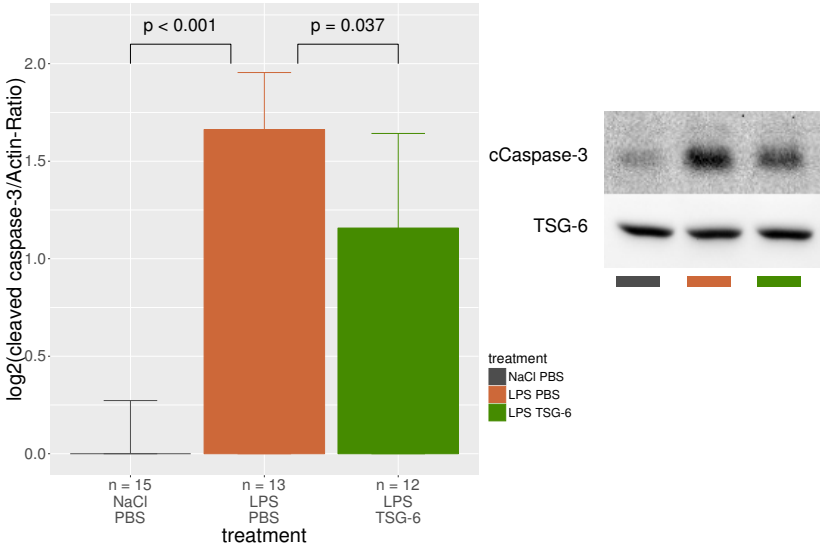

Figure 3.11.: **Levels of cleaved caspase-3 under inflammatory conditions and TSG-6 treatment**
Cleaved caspase-3 levels in newborn rat brains are increased after LPS injection. Additional TSG-6 treatment reduces this elevation by about 30%.
Method: Western blot, *samples:* hemispheres/n = 12-15, *treatment:* NaCl = sodium chloride 0.9% [P3]/LPS = lipopolysaccharide 0.25 mg/kg [P3]/TSG-6 = TSG-6 2.25 mg/kg 2x/d [P3+P4]/PBS = phosphate buffered saline 2x/d [P3+P4]/decapitation on P5, *graphics:* bar plots + CI, *statistics:* pairwise t-test

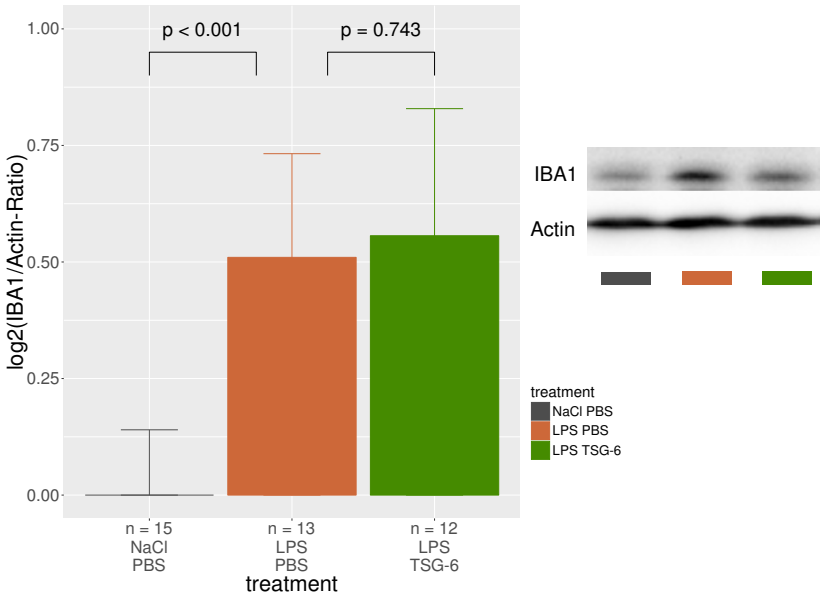

Figure 3.12.: **Expression of Iba1 under inflammatory conditions and TSG-6 treatment**
Iba1 expression in newborn rat brains, a marker for microglia activation, is increased after LPS injection. Additional TSG-6 treatment does not alter the level of expression.
Method: Western blot, *samples:* hemispheres/n = 12-15, *treatment:* NaCl = sodium chloride 0.9% [P3]/LPS = lipopolysaccharide 0.25 mg/kg [P3]/TSG-6 = TSG-6 2.25 mg/kg 2x/d [P3+P4]/PBS = phosphate buffered saline 2x/d [P3+P4]/decapitation on P5, *graphics:* bar plots + CI, *statistics:* pairwise t-test

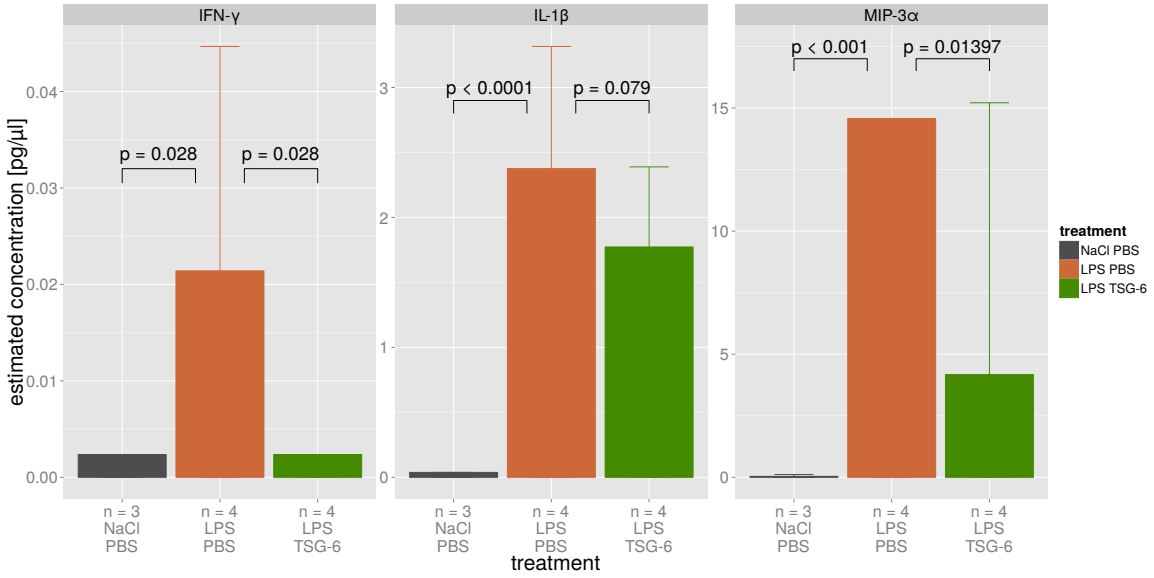

Figure 3.13.: **Systemic inflammatory response after inflammatory stimulus and TSG-6 treatment**
Cytokine expression is elevated in serum 6 h after inflammatory stimulus. Additional TSG-6 treatment reduces the elevated levels.
Method: multiplex ELISA, *samples:* serum/n = 3-4, *treatment:* NaCl = sodium chloride 0.9% [P3]/LPS = lipopolysaccharide 0.25 mg/kg [P3]/TSG-6 = TSG-6 2.25 mg/kg 2x/d [P3+P4]/PBS = phosphate buffered saline 2x/d [P3+P4]/decapitation on P3+6 h, *graphics:* bar plots + CI, *statistics:* pairwise t-test

4. Discussion

4.1. Role of TSG-6 in the developing brain

TSG-6 expression in the first postnatal days of brain development at both mRNA and protein levels (figure 3.1, figure 3.2) suggests that TSG-6 may be important during brain maturation. The linear up-regulation of TSG-6 mRNA between P1 and P15 in whole brain hemispheres and the different levels of expression in hemispheres, cortex, thalamus and striatum implicate a highly regulated mechanism. In contrast, TSG-6 protein levels show profound variability during development from P1 to P15, but it is certainly expressed in the neonatal brain. One possible mechanism of TSG-6 to influence brain development is its capability to modify the extracellular matrix. Baranova et al. revealed that TSG-6 oligomers cross-link and condense hyaluronan matrices *in vitro* under *in vivo* like conditions. Uniaxial stretching has been postulated to transform these matrices to fiber-like structures. Such fiber-like hyaluronan structures have been found along migratory pathways of neuronal precursor cells and in a pericellular pattern around oligodendrocyte precursor cells (Baier et al., 2007; Gerlach et al., 2010), suggesting a role of TSG-6 during migration of neuronal precursor cells and maturation of oligodendrocytes.

Prospects Proving co-localization of TSG-6 with neuronal or oligodendrocyte precursor cells would support this hypothesis, but despite trying several antibodies, we did not achieve a convincing immunohistochemical staining of TSG-6. Another approach would be investigating TSG-6 knock out animals. TSG-$6^{-/-}$ mice have been reported to not display any gross physical or behavioural abnormalities, but detailed behavioural studies are missing. Neither exist investigations about TSG-6 and fibre-like hyaluronan structures in the brain (Fülöp et al., 2003; Szántó et al., 2004).

4.2. Role of TSG-6 in inflammation-induced developmental brain injury

Treatment of neonatal Wistar rats with LPS induces pronounced systemic inflammation with activation of a large number of cytokines, peaking after 2-8 h (figure 3.3). Although *in-vitro* studies of oligodendrocyte-microglia-co-cultures have shown elevated cytokine gene expression after LPS stimulation (Brehmer et al., 2012) and *in-vivo* studies of brain tissue demonstrated elevated cytokine gene and protein expression after IL-1β stimulation (Ådén et al., 2010), we did not detect cytokines in the brain at levels above the detection limit of our multiplex ELISA. However, we were able to show increased microglia activation by detecting

elevated Iba1 levels (figure 3.12, (Boche et al., 2013)). Therefore the lack of cytokine detection in the brain is most likely due to limited sensitivity of the multiplex ELISA technique. Systemic inflammation is followed by a global decrease of cytokines beginning at about 48 h after the inflammatory stimulus (figure 3.4). LPS is known to have a preconditioning effect on second insults like ischaemia/hypoxia in the neonatal brain at certain doses and time intervals between the two insults (Mallard, Hagberg, 2007). A reduction in the expression of cytokines after an inflammatory stimulus may contribute to the preconditioning effect. In contrast, cell counts were still slightly shifted to monocytes (figure 3.6) as a cellular residue of the systemic inflammation (Shi, Pamer, 2011), and thrombocytes were reduced to less than 50% most likely due to impaired platelet production (figure 3.5) (Levi, Schultz, 2010).

As TSG-6 is an endogenous, anti-inflammatory protein that is expressed upon inflammation (Wisniewski et al., 1993; Bayliss et al., 2001; Al'Qteishat et al., 2006), we analysed whether TSG-6 is also up-regulated in the brain under inflammatory conditions. Figure 3.7 shows that TSG-6 gene expression is significantly up-regulated after 4 h and therefore matches the peak of the systemic cytokine response. In comparison to an adult model of cerebral ischaemia, the up-regulation of TSG-6 in our model is lower (Lin et al., 2013). This could either be a characteristic of our model of LPS-induced neuroinflammation or the result of a weaker response due to the immaturity of the neonatal immune system and therefore a characteristic of neonatal neuroinflammation.

4.3. Therapeutic potential of TSG-6 in inflammation-induced developmental brain injury

Cleaved caspase-3 is a downstream effector of apoptosis, with caspase-3 being the final target of several apoptotic pathways. In the brain, it is not only a hallmark of apoptosis but also plays a crucial role in reorganizing axonal and dendritic structures. It contributes to long-term depression (LTD) (Li et al., 2010) and inhibits long-term potentiation (LTP) (Jo et al., 2011). LTD and LTP are an activity-dependent reduction/increase in the efficacy of neuronal synapses following a long patterned stimulus and are discussed to be essential for learning (Sweatt, 2016). While apoptosis is triggered by widespread cleavage and activation of caspase-3 in the whole cell, neuronal plasticity is promoted by limited activation of caspase-3 in dendritic regions (Erturk et al., 2014). Disturbances in these processes can lead to an extensive malfunction of the CNS, especially during development (Hyman, Yuan, 2012; Lakhani, 2006; Kuida et al., 1996). Therefore, reduced activation of caspase-3 after administration of LPS and TSG-6, compared to sole LPS-treatment (figure 3.11) provides first evidence for the neuroprotective potential of TSG-6, raising the question of the underlying mechanism. In principle, a neuroprotective effect could be achieved at multiple time points, starting by inhibiting the initiation of the inflammatory cascade via TLR-4 (Pålsson-McDermott, O'Neill, 2004), up to modulating local inflammatory effects in the brain. In order to get a first indication where TSG-6 might alter our model of inflammation-induced brain damage, we investigated the systemic inflammatory response 6 h after LPS administration. It is substantially reduced after TSG-6 treatment exhibiting significantly reduced amounts of pro-inflammatory cytokines

(IFN-γ, MIP-3α) in serum (figure 3.13). Therefore TSG-6 may impair the inflammatory cascade before it actually reaches the brain. At P5, compared to sole LPS administration, additional TSG-6 did not alter cytokine expression, except of IL-18 expression (figure 3.4). Thrombocytes and immune cell counts were not affected by TSG-6 either (figure 3.6, 3.5). As TSG-6 might as well influence local inflammatory processes in brain, we investigated the expression of Iba1 in the brain, which is a marker for activated microglia (figure 3.12). We detected an increased expression of Iba1 after LPS treatment, which was not affected by additional TSG-6 administration. Still, the consequences of this increased microglia activation remain elusive as Iba1 is just a general marker of activation and does not provide information about the actual phenotype of microglia: M1 (classical activation) and M2 (sometimes subdivided into alternative activation and acquired deactivation) (Boche et al., 2013; Ito et al., 1998).

Prospects This study shows the neuroprotective potential of TSG-6 in inflammation-induced developmental brain injury. Next steps should focus on investigating if reduced apoptosis in the brain actually improves the behavioural outcome. Furthermore, it is still unclear, which pathways TSG-6 modulates to reduce systemic inflammation and if TSG-6 has additional local effects in brain. Figure 4.1 shows possible mechanisms.

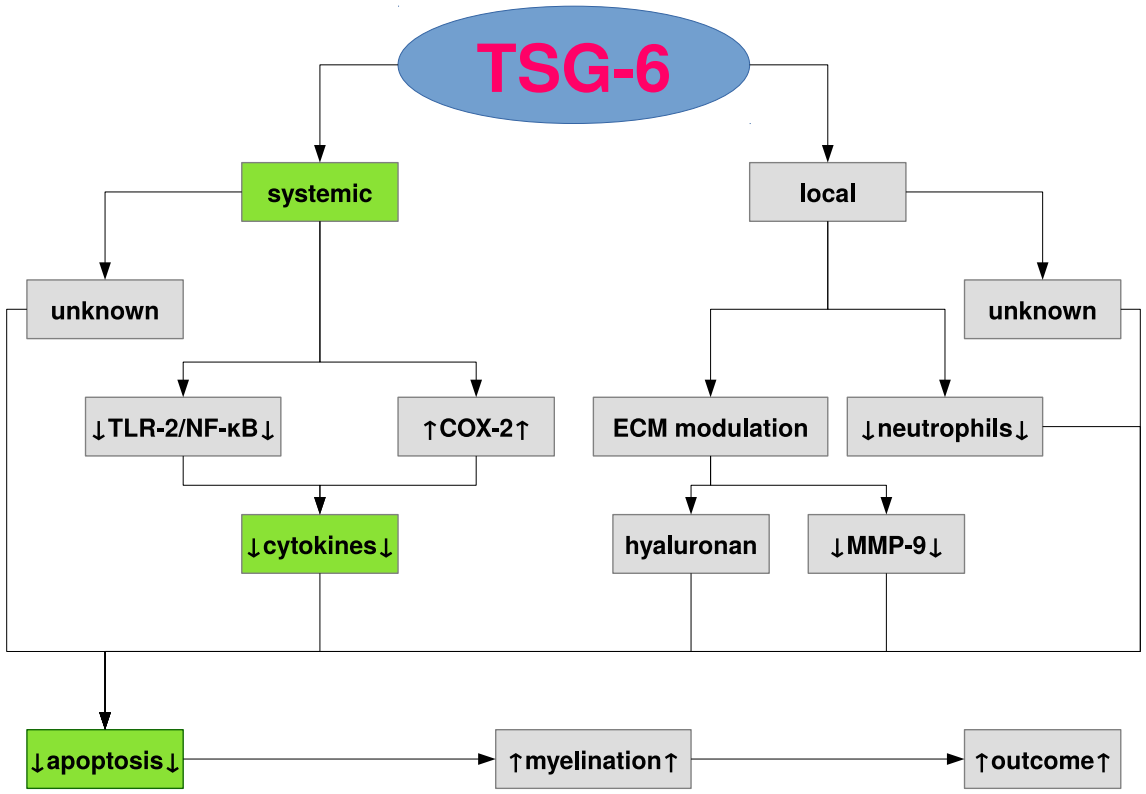

Figure 4.1.: **Molecular pathways of TSG-6**
Known functions of TSG-6 suggest multiple pathways of its anti-inflammatory and neuroprotective effects. Reduced apoptosis might result in better myelination and finally in improved neurological outcome. Green boxes represent results of our study.
TLR-2/NF-κB: TSG-6 inhibits CD-44 dependently the TLR-2 signal cascade limiting the amount of translocated NF-κB into the cell nucleus (Choi et al., 2011). TLR-2 recognizes cell structures of bacteria, including LPS (Godowski et al., 1998).
COX-2: TSG-6 increases COX-2 expression with subsequent secretion of PGD_2 (Mindrescu et al., 2005), which exhibits anti-inflammatory activity (Ricciotti, FitzGerald, 2011).
Hyaluronan: TSG-6 catalyses the formation of Hyaluronan-Heavychain complexes (Rugg et al., 2005; Sanggaard et al., 2008; Sanggaard et al., 2010), creating condensed Hyaluronan matrices in vitro (Baranova et al., 2011).
MMP-9: TSG-6 modulates the anti-plasmin activity of the bikunin domain of inter-α-inhibitor, which is abundant in plasma. Lower plasmin activity leads to lower activity of matrix-metalloproteinases which are involved in matrix degradation (Wisniewski et al., 1996). MMP-9 gene knock-out showed neuroprotection in a model of cerebral hypoxia-ischaemia in the immature brain (Svedin et al., 2007).
Neutrophils: TSG-6 inhibits neutrophil migration (Getting et al., 2002).

5. Conclusion

TSG-6 expression is spatiotemporally regulated in the neonatal brain. It is up-regulated from P1 to P15 and shows varying expression in different brain regions. Therefore, according to its functional characteristics, TSG-6 may play a role in oligodendrocyte maturation and neuronal precursor cell migration. Furthermore, TSG-6 is up-regulated in the neonatal brain under inflammatory conditions. Exogenous administration of rhTSG-6 decreases the systemic inflammation and reduces apoptosis in the brain, indicating a neuroprotective effect.

6. Abstract

Introduction: Inflammation is an important factor contributing to developmental brain injury in preterm infants. Although tumor necrosis factor-inducible gene 6 protein (TSG-6) has immunomodulatory effects in several inflammatory conditions in adult animals, the role of TSG-6 in the developing brain, its impact on perinatal inflammation and its therapeutic potential is currently unknown. The aim of the current work was 1) to characterise the developmental expression of TSG-6 in the newborn rat brain, 2) to evaluate the impact of lipopolysaccharide (LPS) exposure on TSG-6 expression and 3) to assess the therapeutic potential of exogenous TSG-6 administration.

Methods: Brain hemispheres of healthy Wistar rats (postnatal day 1-postnatal day 15 (P1-P15)) were evaluated with regard to the physiological expression of TSG-6. LPS-treated rats (0.25 mg/kg LPS intraperitoneally (i.p.) on P3) were analysed for inflammation-induced changes in TSG-6 and cytokine expression. To evaluate whether exogenous recombinant human (rh)TSG-6 affects inflammation-induced brain injury, Wistar rats exposed to LPS on P3 were treated with rhTSG-6 i.p. (4 repetitive doses of 2.25 mg/kg every 12 h, first dose 3 h before LPS injection).

Results: TSG-6 is physiologically expressed in the developing brain with a linear increase in expression from P1 to P15 at the messenger ribonucleic acid (mRNA) level. At P6, regional differences in TSG-6 expression in the cortex, thalamus and striatum were detected at mRNA and protein level. Furthermore, TSG-6 gene expression was significantly increased by inflammation (induced by LPS treatment). Combined treatment with LPS and TSG-6 vs. LPS exposure alone resulted in significant down-regulation of cleaved caspase-3, a marker of apoptosis and neuronal plasticity. In addition, several inflammatory serum markers were decreased after TSG-6 treatment.

Conclusion: TSG-6 is physiologically expressed in the developing brain. Changes of TSG-6 expression associated with inflammation suggest a role of TSG-6 in neuroinflammation. Reduction of cleaved caspase-3 by TSG-6 treatment demonstrates the putative neuroprotective potential of exogenous TSG-6 administration in inflammation-induced developmental brain injury.

A. Bibliography

1. Ådén, U., G. Favrais, F. Plaisant, M. Winerdal, U. Felderhoff-Mueser, J. Lampa, V. Lelièvre, P. Gressens (2010):

   Systemic inflammation sensitizes the neonatal brain to excitotoxicity through a pro-/anti-inflammatory imbalance: Key role of TNFα pathway and protection by etanercept.

   Brain, Behavior, and Immunity 24, 747–758.

2. Al'Qteishat, A., J. Gaffney, J. Krupinski, F. Rubio, D. West, S. Kumar, P. Kumar, N. Mitsios, M. Slevin (2006):

   Changes in hyaluronan production and metabolism following ischaemic stroke in man.

   Brain 129, 2158–2176.

3. Back, S. A., X. Gan, Y. Li, P. A. Rosenberg, J. J. Volpe (1998):

   Maturation-dependent vulnerability of oligodendrocytes to oxidative stress-induced death caused by glutathione depletion.

   The Journal of neuroscience : the official journal of the Society for Neuroscience 18, 6241–53.

4. Baier, C., S. L. Baader, J. Jankowski, V. Gieselmann, K. Schilling, U. Rauch, J. Kappler (2007):

   Hyaluronan is organized into fiber-like structures along migratory pathways in the developing mouse cerebellum.

   Matrix Biology 26, 348–358.

5. Baranova, N. S., E. Nileback, F. M. Haller, D. C. Briggs, S. Svedhem, A. J. Day, R. P. Richter (2011):

   The Inflammation-associated Protein TSG-6 Cross-links Hyaluronan via Hyaluronan-induced TSG-6 Oligomers.

   Journal of Biological Chemistry 286, 25675–25686.

6. Bayliss, M., S. Howat, J. Dudhia, J. Murphy, F. Barry, J. Edwards, A. Day (2001):

   Up-regulation and differential expression of the hyaluronan-binding protein TSG-6 in cartilage and synovium in rheumatoid arthritis and osteoarthritis.

   Osteoarthritis and Cartilage 9, 42–48.

7. Boche, D., V. H. Perry, J. A. R. Nicoll (2013):

   Review: Activation patterns of microglia and their identification in the human brain.

   Neuropathology and Applied Neurobiology 39, 3–18.

8. Brehmer, F., I. Bendix, S. Prager, Y. van de Looij, B. S. Reinboth, J. Zimmermanns, G. W. Schlager, D. Brait, M. Sifringer, S. Endesfelder, S. Sizonenko, C. Mallard, C. Bührer, U. Felderhoff-Mueser, B. Gerstner (2012):

   Interaction of inflammation and hyperoxia in a rat model of neonatal white matter damage.

   PloS one 7. Ed. by Arai, K., e49023.

9. Burd, I., B. Balakrishnan, S. Kannan (2012):

   Models of Fetal Brain Injury, Intrauterine Inflammation, and Preterm Birth.

   American Journal of Reproductive Immunology 67, 287–294.

10. Castillo-Melendez, M., T. Yawno, G. Jenkin, S. L. Miller (2013):

    Stem cell therapy to protect and repair the developing brain: A review of mechanisms of action of cord blood and amnion epithelial derived cells.

    Frontiers in Neuroscience 7, 194.

11. Choi, H., R. H. Lee, N. Bazhanov, J. Y. Oh, D. J. Prockop (2011):

    Anti-inflammatory protein TSG-6 secreted by activated MSCs attenuates zymosan-induced mouse peritonitis by decreasing TLR2/NF-κB signaling in resident macrophages.

    Blood 118, 330–338.

12. Danchuk, S., J. H. Ylostalo, F. Hossain, R. Sorge, A. Ramsey, R. W. Bonvillain, J. A. Lasky, B. A. Bunnell, D. A. Welsh, D. J. Prockop, D. E. Sullivan (2011):

    Human multipotent stromal cells attenuate lipopolysaccharide-induced acute lung injury in mice via secretion of tumor necrosis factor-α-induced protein 6.

    Stem Cell Research & Therapy 2, 27.

13. Degos, V., G. Favrais, A. M. Kaindl, S. Peineau, A. M. Guerrot, C. Verney, P. Gressens (2010):

    Inflammation processes in perinatal brain damage.

    Journal of Neural Transmission 117, 1009–1017.

14. Deng, W. (2010):

    Neurobiology of injury to the developing brain.

    Nature Reviews Neurology 6, 328–336.

15. Dobbing, J., J. Sands (1979):

    Comparative aspects of the brain growth spurt.

    Early human development 3, 79–83.

16. Erturk, A., Y. Wang, M. Sheng (2014):

Local Pruning of Dendrites and Spines by Caspase-3-Dependent and Proteasome-Limited Mechanisms.

Journal of Neuroscience 34, 1672–1688.

17. Favrais, G., P. Tourneux, E. Lopez, X. Durrmeyer, G. Gascoin, D. Ramful, E. Zana-Taieb, O. Baud (2014):

Impact of Common Treatments Given in the Perinatal Period on the Developing Brain.

Neonatology 106, 163–172.

18. Fong, Y., K. Sebestyen (2013):

nCal: Nonlinear Calibration.

19. Fry, M., A. V. Ferguson (2007):

The sensory circumventricular organs: Brain targets for circulating signals controlling ingestive behavior.

Physiology & Behavior 91, 413–423.

20. Fülöp, C., R. V. Kamath, Y. Li, J. M. Otto, A. Salustri, B. R. Olsen, T. T. Glant, V. C. Hascall (1997):

Coding sequence, exon-intron structure and chromosomal localization of murine TNF-stimulated gene 6 that is specifically expressed by expanding cumulus cell-oocyte complexes.

Gene 202, 95–102.

21. Fülöp, C., S. Szántó, D. Mukhopadhyay, T. Bárdos, R. V. Kamath, M. S. Rugg, A. J. Day, A. Salustri, V. C. Hascall, T. T. Glant, K. Mikecz (2003):

Impaired cumulus mucification and female sterility in tumor necrosis factor-induced protein-6 deficient mice.

Development 130, 2253–2261.

22. Gerlach, D., T. Kaminski, F. Pérez-Willard, G. Kirfel, V. Gieselmann, J. Kappler (2010):

Nanofibers in a hyaluronan-based pericellular matrix.

Matrix Biology 29, 664–667.

23. Getting, S. J., D. J. Mahoney, T. Cao, M. S. Rugg, E. Fries, C. M. Milner, M. Perretti, A. J. Day (2002):

The link module from human TSG-6 inhibits neutrophil migration in a hyaluronan- and inter-α-inhibitor-independent manner.

Journal of Biological Chemistry 277, 51068–51076.

24. Gill, S. V., T. a. May-Benson, A. Teasdale, E. G. Munsell (2013):

Birth and developmental correlates of birth weight in a sample of children with potential sensory processing disorder.

BMC pediatrics 13, 29.

25. Godowski, P. J., R.-B. Yang, M. R. Mark, A. Gray, A. Huang, M. H. Xie, M. Zhang, A. Goddard, W. I. Wood, A. L. Gurney (1998):

Toll-like receptor-2 mediates lipopolysaccharide-induced cellular signalling.

Nature 395, 284–288.

26. Goldenberg, R. L., J. F. Culhane, J. D. Iams, R. Romero (2008):

Epidemiology and causes of preterm birth.

The Lancet 371, 75–84.

27. Haastert, I. C. van, F. Groenendaal, C. S. P. Uiterwaal, J. U. Termote, M. van der Heide-Jalving, M. J. Eijsermans, J. W. Gorter, P. J. Helders, M. J. Jongmans, L. S. de Vries (2011):

Decreasing Incidence and Severity of Cerebral Palsy in Prematurely Born Children.

The Journal of Pediatrics 159, 86–91.e1.

28. Hagberg, H., P. Gressens, C. Mallard (2012):

Inflammation during fetal and neonatal life: Implications for neurologic and neuropsychiatric disease in children and adults.

Annals of Neurology 71, 444–457.

29. Hagberg, H., C. Mallard (2005):

Effect of inflammation on central nervous system development and vulnerability.

Current opinion in neurology 18, 117–23.

30. Hagberg, H., C. Mallard, D. M. Ferriero, S. J. Vannucci, S. W. Levison, Z. S. Vexler, P. Gressens (2015):

The role of inflammation in perinatal brain injury.

Nature Reviews Neurology 11, 192–208.

31. Himmelmann, K., G. Hagberg, P. Uvebrant (2010):

The changing panorama of cerebral palsy in Sweden. X. Prevalence and origin in the birth-year period 1999-2002.

Acta Paediatrica 99, 1337–1343.

32. Hyman, B. T., J. Yuan (2012):

Apoptotic and non-apoptotic roles of caspases in neuronal physiology and pathophysiology.

Nature Reviews Neuroscience 13, 395–406.

33. Ito, D., Y. Imai, K. Ohsawa, K. Nakajima, Y. Fukuuchi, S. Kohsaka (1998):

Microglia-specific localisation of a novel calcium binding protein, Iba1.

Brain research. Molecular brain research 57, 1–9.

34. Jo, J., D. J. Whitcomb, K. M. Olsen, T. L. Kerrigan, S.-C. Lo, G. Bru-Mercier, B. Dickinson, S. Scullion, M. Sheng, G. Collingridge, K. Cho (2011):

Aβ1–42 inhibition of LTP is mediated by a signaling pathway involving caspase-3, Akt1 and GSK-3β.

Nature Neuroscience 14, 545–547.

35. Jobe, A. H., E. Bancalari (2001):

Bronchopulmonary dysplasia.

American journal of respiratory and critical care medicine 163, 1723–9.

36. Keller, M., U. Felderhoff-Mueser, H. Lagercrantz, O. Dammann, N. Marlow, P. Hüppi, G. Buonocore, C. Poets, G. Simbruner, H. Guimaraes, S. Mader, M. Merialdi, O. D. Saugstad (2010):

Policy benchmarking report on neonatal health and social policies in 13 European countries.

Acta Paediatrica 99, 1624–1629.

37. Kramer, M. S., K. Demissie, H. Yang, R. W. Platt, R. Sauvé, R. Liston (2000):

The contribution of mild and moderate preterm birth to infant mortality. Fetal and Infant Health Study Group of the Canadian Perinatal Surveillance System.

JAMA 284, 843–9.

38. Kuida, K., T. S. Zheng, S. Na, C.-Y. Kuan, D. Yang, H. Karasuyama, P. Rakic, R. A. Flavell (1996):

Decreased apoptosis in the brain and premature lethality in CPP32-deficient mice.

Nature 384, 368–372.

39. Lakhani, S. A. (2006):

Caspases 3 and 7: Key Mediators of Mitochondrial Events of Apoptosis.

Science 311, 847–851.

40. Larroque, B., P.-Y. Ancel, S. Marret, L. Marchand, M. André, C. Arnaud, V. Pierrat, J.-C. Rozé, J. Messer, G. Thiriez, A. Burguet, J.-C. Picaud, G. Bréart, M. Kaminski (2008):

Neurodevelopmental disabilities and special care of 5-year-old children born before 33 weeks of gestation (the EPIPAGE study): a longitudinal cohort study.

The Lancet 371, 813–820.

41. Lawn, J. E., S. Cousens, J. Zupan (2005):

    4 million neonatal deaths: When? Where? Why?

    The Lancet 365, 891–900.

42. Lawn, J. E., R. Davidge, V. K. Paul, S. von Xylander, J. de Graft Johnson, A. Costello, M. V. Kinney, J. Segre, L. Molyneux (2013):

    Born too soon: care for the preterm baby.

    Reproductive health 10 Suppl 1, S5.

43. Lawn, J. E., K. Wilczynska-Ketende, S. N. Cousens (2006):

    Estimating the causes of 4 million neonatal deaths in the year 2000.

    International journal of epidemiology 35, 706–18.

44. Lee, R. H., A. A. Pulin, M. J. Seo, D. J. Kota, J. Ylostalo, B. L. Larson, L. Semprun-Prieto, P. Delafontaine, D. J. Prockop (2009):

    Intravenous hMSCs Improve Myocardial Infarction in Mice because Cells Embolized in Lung Are Activated to Secrete the Anti-inflammatory Protein TSG-6.

    Cell Stem Cell 5, 54–63.

45. Lee, T. H., G. W. Lee, E. B. Ziff, J. Vilcek (1990):

    Isolation and characterization of eight tumor necrosis factor-induced gene sequences from human fibroblasts.

    Molecular and cellular biology 10, 1982–8.

46. Levi, M., M. Schultz (2010):

    Coagulopathy and platelet disorders in critically ill patients.

    Minerva anestesiologica 76, 851–9.

47. Li, Z., J. Jo, J.-M. Jia, S.-C. Lo, D. J. Whitcomb, S. Jiao, K. Cho, M. Sheng (2010):

    Caspase-3 Activation via Mitochondria Is Required for Long-Term Depression and AMPA Receptor Internalization.

    Cell 141, 859–871.

48. Lin, Q.-m., S. Zhao, L.-L. Zhou, X.-S. Fang, Y. Fu, Z.-T. Huang (2013):

    Mesenchymal stem cells transplantation suppresses inflammatory responses in global cerebral ischemia: contribution of TNF-α-induced protein 6.

    Acta Pharmacologica Sinica 34, 784–792.

49. Liu, X.-B., Y. Shen, J. M. Plane, W. Deng (2013):

    Vulnerability of premyelinating oligodendrocytes to white-matter damage in neonatal brain injury.

    Neuroscience Bulletin 29, 229–238.

50. Livak, K. J., T. D. Schmittgen (2001):

Analysis of Relative Gene Expression Data Using Real-Time Quantitative PCR and the 2−ΔΔCT Method.

Methods 25, 402–408.

51. Mallard, C., H. Hagberg (2007):

Inflammation-induced preconditioning in the immature brain.

Seminars in Fetal and Neonatal Medicine 12, 280–286.

52. Milner, C. M., A. J. Day (2003):

TSG-6: a multifunctional protein associated with inflammation.

Journal of cell science 116, 1863–73.

53. Milner, C., V. Higman, A. Day (2006):

TSG-6: a pluripotent inflammatory mediator?

Biochemical Society Transactions 34, 446–450.

54. Mindrescu, C., J. Le, H.-G. Wisniewski, J. Vilcek (2005):

Up-regulation of cyclooxygenase-2 expression by TSG-6 protein in macrophage cell line.

Biochemical and Biophysical Research Communications 330, 737–745.

55. Murray, C. J. L., T. Vos, R. Lozano, M. Naghavi, A. D. Flaxman, C. Michaud, M. Ezzati, K. Shibuya, J. A. Salomon, S. Abdalla, V. Aboyans, J. Abraham, I. Ackerman, R. Aggarwal, S. Y. Ahn, M. K. Ali, M. A. AlMazroa, M. Alvarado, H. R. Anderson, L. M. Anderson, K. G. Andrews, C. Atkinson, L. M. Baddour, A. N. Bahalim, S. Barker-Collo, L. H. Barrero, D. H. Bartels, M.-G. Basáñez, A. Baxter, M. L. Bell, E. J. Benjamin, D. Bennett, E. Bernabé, K. Bhalla, B. Bhandari, B. Bikbov, A. B. Abdulhak, G. Birbeck, J. A. Black, H. Blencowe, J. D. Blore, F. Blyth, I. Bolliger, A. Bonaventure, S. Boufous, R. Bourne, M. Boussinesq, T. Braithwaite, C. Brayne, L. Bridgett, S. Brooker, P. Brooks, T. S. Brugha, C. Bryan-Hancock, C. Bucello, R. Buchbinder, G. Buckle, C. M. Budke, M. Burch, P. Burney, R. Burstein, B. Calabria, B. Campbell, C. E. Canter, H. Carabin, J. Carapetis, L. Carmona, C. Cella, F. Charlson, H. Chen, A. T.-A. Cheng, D. Chou, S. S. Chugh, L. E. Coffeng, S. D. Colan, S. Colquhoun, K. E. Colson, J. Condon, M. D. Connor, L. T. Cooper, M. Corriere, M. Cortinovis, K. C. de Vaccaro, W. Couser, B. C. Cowie, M. H. Criqui, M. Cross, K. C. Dabhadkar, M. Dahiya, N. Dahodwala, J. Damsere-Derry, G. Danaei, A. Davis, D. D. Leo, L. Degenhardt, R. Dellavalle, A. Delossantos, J. Denenberg, S. Derrett, D. C. Des Jarlais, S. D. Dharmaratne, M. Dherani, C. Diaz-Torne, H. Dolk, E. R. Dorsey, T. Driscoll, H. Duber, B. Ebel, K. Edmond, A. Elbaz, S. E. Ali, H. Erskine, P. J. Erwin, P. Espindola, S. E. Ewoigbokhan, F. Farzadfar, V. Feigin, D. T. Felson, A. Ferrari, C. P. Ferri, E. M. Fèvre, M. M. Finucane, S. Flaxman, L. Flood, K. Foreman, M. H. Forouzanfar, F. G. R. Fowkes, M. Fransen, M. K. Freeman, B. J. Gabbe, S. E.

Gabriel, E. Gakidou, H. A. Ganatra, B. Garcia, F. Gaspari, R. F. Gillum, G. Gmel, D. Gonzalez-Medina, R. Gosselin, R. Grainger, B. Grant, J. Groeger, F. Guillemin, D. Gunnell, R. Gupta, J. Haagsma, H. Hagan, Y. A. Halasa, W. Hall, D. Haring, J. M. Haro, J. E. Harrison, R. Havmoeller, R. J. Hay, H. Higashi, C. Hill, B. Hoen, H. Hoffman, P. J. Hotez, D. Hoy, J. J. Huang, S. E. Ibeanusi, K. H. Jacobsen, S. L. James, D. Jarvis, R. Jasrasaria, S. Jayaraman, N. Johns, J. B. Jonas, G. Karthikeyan, N. Kassebaum, N. Kawakami, A. Keren, J.-P. Khoo, C. H. King, L. M. Knowlton, O. Kobusingye, A. Koranteng, R. Krishnamurthi, F. Laden, R. Lalloo, L. L. Laslett, T. Lathlean, J. L. Leasher, Y. Y. Lee, J. Leigh, D. Levinson, S. S. Lim, E. Limb, J. K. Lin, M. Lipnick, S. E. Lipshultz, W. Liu, M. Loane, S. L. Ohno, R. Lyons, J. Mabweijano, M. F. MacIntyre, R. Malekzadeh, L. Mallinger, S. Manivannan, W. Marcenes, L. March, D. J. Margolis, G. B. Marks, R. Marks, A. Matsumori, R. Matzopoulos, B. M. Mayosi, J. H. McAnulty, M. M. McDermott, N. McGill, J. McGrath, M. E. Medina-Mora, M. Meltzer, Z. A. Memish, G. A. Mensah, T. R. Merriman, A.-C. Meyer, V. Miglioli, M. Miller, T. R. Miller, P. B. Mitchell, C. Mock, A. O. Mocumbi, T. E. Moffitt, A. A. Mokdad, L. Monasta, M. Montico, M. Moradi-Lakeh, A. Moran, L. Morawska, R. Mori, M. E. Murdoch, M. K. Mwaniki, K. Naidoo, M. N. Nair, L. Naldi, K. M. V. Narayan, P. K. Nelson, R. G. Nelson, M. C. Nevitt, C. R. Newton, S. Nolte, P. Norman, R. Norman, M. O'Donnell, S. O'Hanlon, C. Olives, S. B. Omer, K. Ortblad, R. Osborne, D. Ozgediz, A. Page, B. Pahari, J. D. Pandian, A. P. Rivero, S. B. Patten, N. Pearce, R. P. Padilla, F. Perez-Ruiz, N. Perico, K. Pesudovs, D. Phillips, M. R. Phillips, K. Pierce, S. Pion, G. V. Polanczyk, S. Polinder, C. A. Pope, S. Popova, E. Porrini, F. Pourmalek, M. Prince, R. L. Pullan, K. D. Ramaiah, D. Ranganathan, H. Razavi, M. Regan, J. T. Rehm, D. B. Rein, G. Remuzzi, K. Richardson, F. P. Rivara, T. Roberts, C. Robinson, F. R. De Leòn, L. Ronfani, R. Room, L. C. Rosenfeld, L. Rushton, R. L. Sacco, S. Saha, U. Sampson, L. Sanchez-Riera, E. Sanman, D. C. Schwebel, J. G. Scott, M. Segui-Gomez, S. Shahraz, D. S. Shepard, H. Shin, R. Shivakoti, D. Silberberg, D. Singh, G. M. Singh, J. A. Singh, J. Singleton, D. A. Sleet, K. Sliwa, E. Smith, J. L. Smith, N. J. Stapelberg, A. Steer, T. Steiner, W. A. Stolk, L. J. Stovner, C. Sudfeld, S. Syed, G. Tamburlini, M. Tavakkoli, H. R. Taylor, J. A. Taylor, W. J. Taylor, B. Thomas, W. M. Thomson, G. D. Thurston, I. M. Tleyjeh, M. Tonelli, J. A. Towbin, T. Truelsen, M. K. Tsilimbaris, C. Ubeda, E. A. Undurraga, M. J. van der Werf, J. van Os, M. S. Vavilala, N. Venketasubramanian, M. Wang, W. Wang, K. Watt, D. J. Weatherall, M. A. Weinstock, R. Weintraub, M. G. Weisskopf, M. M. Weissman, R. A. White, H. Whiteford, N. Wiebe, S. T. Wiersma, J. D. Wilkinson, H. C. Williams, S. R. Williams, E. Witt, F. Wolfe, A. D. Woolf, S. Wulf, P.-H. Yeh, A. K. Zaidi, Z.-J. Zheng, D. Zonies, A. D. Lopez (2012):

Disability-adjusted life years (DALYs) for 291 diseases and injuries in 21 regions, 1990–2010: a systematic analysis for the Global Burden of Disease Study 2010.

The Lancet 380, 2197–2223.

56. Oh, J. Y., G. W. Roddy, H. Choi, R. H. Lee, J. H. Ylostalo, R. H. Rosa, D. J. Prockop (2010):

Anti-inflammatory protein TSG-6 reduces inflammatory damage to the cornea following chemical and mechanical injury.

Proceedings of the National Academy of Sciences 107, 16875–16880.

57. Oka, A., M. J. Belliveau, P. A. Rosenberg, J. J. Volpe (1993):

Vulnerability of oligodendroglia to glutamate: pharmacology, mechanisms, and prevention.

The Journal of neuroscience : the official journal of the Society for Neuroscience 13, 1441–53.

58. Pålsson-McDermott, E. M., L. A. J. O'Neill (2004):

Signal transduction by the lipopolysaccharide receptor, Toll-like receptor-4.

Immunology 113, 153–62.

59. Prager, S., B. B. Singer, I. Bendix, G. W. Schlager, F. Bertling, B. Ceylan, M. Keller, U. Felderhoff-Mueser, S. Ergün (2013):

CEACAM1 Expression in Oligodendrocytes of the Developing Rat Brain Shows a Spatiotemporal Relation to Myelination and Is Altered in a Model of Encephalopathy of Prematurity.

Developmental Neuroscience 35, 226–240.

60. Quan, N., E. L. Stern, M. B. Whiteside, M. Herkenham (1999):

Induction of pro-inflammatory cytokine mRNAs in the brain after peripheral injection of subseptic doses of lipopolysaccharide in the rat.

Journal of neuroimmunology 93, 72–80.

61. Rees, S., T. Inder (2005):

Fetal and neonatal origins of altered brain development.

Early Human Development 81, 753–761.

62. Ricciotti, E., G. A. FitzGerald (2011):

Prostaglandins and Inflammation.

Arteriosclerosis, Thrombosis, and Vascular Biology 31, 986–1000.

63. Richards, J. S. (2005):

Ovulation: New factors that prepare the oocyte for fertilization.

Molecular and Cellular Endocrinology 234, 75–79.

64. Ritz, C., J. C. Streibig (2005):

Bioassay Analysis using R.

Journal of Statistical Software 12.

65. Romero, R., J. Espinoza, J. Kusanovic, F. Gotsch, S. Hassan, O. Erez, T. Chaiworapongsa, M. Mazor (2006):

The preterm parturition syndrome.

BJOG: An International Journal of Obstetrics & Gynaecology 113, 17–42.

66. Romero, R., J. Espinoza, L. F. Gonçalves, J. P. Kusanovic, L. Friel, S. Hassan (2007):

The role of inflammation and infection in preterm birth.

Seminars in reproductive medicine 25, 21–39.

67. Rugg, M. S., A. C. Willis, D. Mukhopadhyay, V. C. Hascall, E. Fries, C. Fülöp, C. M. Milner, A. J. Day (2005):

Characterization of Complexes Formed between TSG-6 and Inter-α-inhibitor That Act as Intermediates in the Covalent Transfer of Heavy Chains onto Hyaluronan.

Journal of Biological Chemistry 280, 25674–25686.

68. Saigal, S., L. W. Doyle (2008):

An overview of mortality and sequelae of preterm birth from infancy to adulthood.

The Lancet 371, 261–269.

69. Sanggaard, K. W., C. Scavenius, A. J. Rasmussen, H.-G. Wisniewski, I. B. Thogersen, J. J. Enghild (2010):

The TSG-6/HC2-mediated Transfer Is a Dynamic Process Shuffling Heavy Chains between Glycosaminoglycans.

Journal of Biological Chemistry 285, 21988–21993.

70. Sanggaard, K. W., C. S. Sonne-Schmidt, T. P. Krogager, K. A. Lorentzen, H.-G. Wisniewski, I. B. Thogersen, J. J. Enghild (2008):

The Transfer of Heavy Chains from Bikunin Proteins to Hyaluronan Requires Both TSG-6 and HC2.

Journal of Biological Chemistry 283, 18530–18537.

71. Semple, B. D., K. Blomgren, K. Gimlin, D. M. Ferriero, L. J. Noble-Haeusslein (2013):

Brain development in rodents and humans: Identifying benchmarks of maturation and vulnerability to injury across species.

Progress in neurobiology 106-107, 1–16.

72. Shi, C., E. G. Pamer (2011):

Monocyte recruitment during infection and inflammation.

Nature Reviews Immunology 11, 762–774.

73. Shi, S.-R., Y. Shi, C. R. Taylor (2011):

Antigen retrieval immunohistochemistry: review and future prospects in research and diagnosis over two decades.

The journal of histochemistry and cytochemistry : official journal of the Histochemistry Society 59, 13–32.

74. Svedin, P., H. Hagberg, K. Savman, C. Zhu, C. Mallard (2007):

Matrix Metalloproteinase-9 Gene Knock-out Protects the Immature Brain after Cerebral Hypoxia-Ischemia.

Journal of Neuroscience 27, 1511–1518.

75. Sweatt, J. D. (2016):

Neural Plasticity & Behavior - Sixty Years of Conceptual Advances.

Journal of neurochemistry.

76. Szántó, S., T. Bárdos, I. Gál, T. T. Glant, K. Mikecz (2004):

Enhanced neutrophil extravasation and rapid progression of proteoglycan-induced arthritis in TSG-6-knockout mice.

Arthritis & Rheumatism 50, 3012–3022.

77. Tan, K., D. McGrouther, A. Day, C. Milner, A. Bayat (2011):

Characterization of hyaluronan and TSG-6 in skin scarring: differential distribution in keloid scars, normal scars and unscarred skin.

Journal of the European Academy of Dermatology and Venereology 25, 317–327.

78. Team, R. C., R Core Team (2012):

R: A Language and Environment for Statistical Computing.

Vienna, Austria.

79. Villar, J., A. T. Papageorghiou, H. E. Knight, M. G. Gravett, J. Iams, S. A. Waller, M. Kramer, J. F. Culhane, F. C. Barros, A. Conde-Agudelo, Z. A. Bhutta, R. L. Goldenberg (2012):

The preterm birth syndrome: a prototype phenotypic classification.

American Journal of Obstetrics and Gynecology 206, 119–123.

80. Virchow, R. (1867):

Congenitale Encephalitis und Myelitis.

Virchows Archiv 38, 129–138.

81. Volpe, J. J. (2009):

The Encephalopathy of Prematurity—Brain Injury and Impaired Brain Development Inextricably Intertwined.

Seminars in Pediatric Neurology 16, 167–178.

82. Volpe, J. J. (2011):

Systemic inflammation, oligodendroglial maturation, and the encephalopathy of prematurity.

Annals of neurology 70, 525–9.

83. Warnes, G. R., with contributions from Ben Bolker, G. Gorjanc, G. Grothendieck, A. Korosec, T. Lumley, D. MacQueen, A. Magnusson, J. Rogers, et al. (2012):

gdata: Various R programming tools for data manipulation.

84. Wen, S. W., G. Smith, Q. Yang, M. Walker (2004):

Epidemiology of preterm birth and neonatal outcome.

Seminars in Fetal and Neonatal Medicine 9, 429–435.

85. Wickham, H. (2009):

ggplot2: elegant graphics for data analysis.

Springer New York.

86. Wickham, H. (2012):

stringr: Make it easier to work with strings.

87. Wisniewski, H. G., J. C. Hua, D. M. Poppers, D. Naime, J. Vilcek, B. N. Cronstein (1996):

TNF/IL-1-inducible protein TSG-6 potentiates plasmin inhibition by inter-α-inhibitor and exerts a strong anti-inflammatory effect in vivo.

Journal of Immunology 156, 1609–15.

88. Wisniewski, H. G., R. Maier, M. Lotz, S. Lee, L. Klampfer, T. H. Lee, J. Vilcek (1993):

TSG-6: a TNF-, IL-1-, and LPS-inducible secreted glycoprotein associated with arthritis.

Journal of Immunology 151, 6593–601.

89. Wu, Y. W., J. M. Colford (2000):

Chorioamnionitis as a risk factor for cerebral palsy: A meta-analysis.

JAMA 284, 1417–24.

90. Zeitlin, J., B. N. Manktelow, A. Piedvache, M. Cuttini, E. Boyle, A. van Heijst, J. Gadzinowski, P. Van Reempts, L. Huusom, T. Weber, S. Schmidt, H. Barros, D. Dillalo, L. Toome, M. Norman, B. Blondel, M. Bonet, E. S. Draper, R. F. Maier, EPICE Research Group (2016):

Use of evidence based practices to improve survival without severe morbidity for very preterm infants: results from the EPICE population based cohort.

BMJ (Clinical research ed.) 354, i2976.

B. List of Tables

C. List of Figures

D. Nomenclature

AMPA α-amino-3-hydroxy-5-methyl-4-isoxazolepropionic acid
APR Acute-phase liver response
APS Ammonium Persulfate
BBB Blood brain barrier
BCA Bicinchoninic acid assay
BSA Bovine serum albumin
CD Cluster of differentiation
CNS Central nervous system
CVO circumventricular organs
DAB 3,3'-Diaminobenzidine
DAPI 4',6-diamidino-2-phenylindole
dNTPs desoxynucleosidetriphosphates
ELBW Extremely Low Birth Weight
GAPDH Glyceraldehyde 3-phosphate dehydrogenase
HE Hematoxylin and eosin stain
IgG Immunoglobulin G
IHC Immunohistochemistry
IL-1 Interleukin-1
IL-1β Interleukin 1β
IL-6 Interleukin-6
IUGR Intrauterine Growth Restriction
LBP LPS-binding protein
LBW Low Birth Weight
LPS Lipopolysaccharide
LTD long-term depression
LTP long-term potentiation
MD-2 Myeloid Differentiation Protein-2
MIAC Microbial invasion of the amniotic cavity
MP Milk powder
MSC Mesenchymal stem cell
NMR neonatal mortality rate
PBS Phosphat buffered saline
preOLGs Pre-oligodendrocytes
PVL Periventricular Leukomalacia
rhTSG-6 recombinant human Tumor necrosis factor stimulated gene 6 protein
RIPA Radio-Immunoprecipitation Assay

RNA Ribonucleic acid
SA-PE Streptavidin Phycoerythrin
SDS Sodium dodecyl sulfate
SGA Small For Gestational Age
TBS Tris buffered saline
TBS-T Tris buffered saline with Tween
TEMED Tetramethylethylenediamine
TLR Toll-like receptor
TNF-α Tumor necrosis factor α
TSG-6 Tumor-necrosis factor inducible gene 6
VLBW Very Low Birth Weight
WB Western blot

E. Acknowledgement

Während meiner Arbeit an dieser Dissertation konnte ich stets auf die Hilfe vieler Personen bauen, ohne die das Projekt nicht möglich gewesen wäre. Insbesondere und zuallererst möchte ich hier Dr. med. Sebastian Prager nennen, der in den letzten Jahren nicht nur ein unverzichtbarer Bestandteil des Teams hinter dieser Arbeit wurde, sondern auch zu einem guten Freund. Sein unermüdliches Engagement kann ich nicht genug hervorheben. So konnte ich selbst am Wochenende gegen Mitternacht mit seiner Unterstützung rechnen, wenn die Tiere unsere Aufmerksamkeit benötigten. Des Weiteren habe ich mit dem gesamten Laborteam eine familiäre und doch ehrgeizige Arbeitsumgebung gefunden, die jedem Mitarbeiter Raum zur individuellen Entfaltung gegeben hat. Vielen Dank dafür, Dr. rer. medic. Ivo Bendix, Dr. med. Karla Drommelschmidt, Ralf Herrmann, Mandana Rizazad, Karina Kempe. Außerdem möchte ich Prof. Hans-Georg Wisniewski und seinem Team danken, die uns ohne finanzielle Interessen mit rhTSG-6 versorgten und uns wertvolle Informationen zur Arbeit mit TSG-6 gaben. Weiterhin danke ich dem Labor der Transfusionsmedizin für die Bereitstellung des Luminex 200, insbesondere Anja König, die bei Fragestellungen immer ansprechbar war. Ebenfalls dankbar bin ich Gabriele Walde aus dem hämatologisch-onkologischen Labor für die Untersuchung der Blutausstriche. Nicht zuletzt danke ich Univ.-Prof. Dr. med. Ursula Felderhoff-Müser und Prof. Dr. med. Matthias Keller für die initiale Idee dieses Projektes und das Vertrauen in mich, dieses Projekt durchführen zu dürfen. Sie standen mir immer bei Fragen zum Projekt als auch zu meiner persönlichen Zukunft zur Verfügung. Zum Schluss danke ich meinen Eltern, Wolfgang und Inge Bertling und meinen Geschwistern, Maren Methling und Niklas Bertling, der besten Familie, die ich mir vorstellen kann. Meine Interessen und Wünsche wurden immer außergewöhnlich gefördert und selbst bei Rückschlägen standen sie mir immer verlässlich zur Seite.

Der Lebenslauf ist in der Online-Version aus Gründen des Datenschutzes nicht enthalten.